Yung Wai-Shing (Orcid ID: 0000-0001-8299-7374)
Lam Hon-Ming (Orcid ID: 0000-0002-6673-8740)

Priming-induced alterations in histone modifications modulate transcriptional responses in soybean under salt stress

Wai-Shing Yung[1, †], Qianwen Wang[1, †], Mingkun Huang[1], Fuk-Ling Wong[1], Ailin Liu[1], Ming-Sin Ng[1], Kwan-Pok Li[1], Ching-Ching Sze[1], Man-Wah Li[1, *], Hon-Ming Lam[1, *]

[1] Centre for Soybean Research of the State Key Laboratory of Agrobiotechnology and School of Life Sciences, The Chinese University of Hong Kong, Shatin, Hong Kong SAR, PR China
Address: Room EG02, Science Centre East Block, The Chinese University of Hong Kong
Shatin, Hong Kong SAR, PR China.

[†] These authors contributed equally to this work.

[*] Corresponding authors:
Hon-Ming Lam; Tel: +852 3943 6336; Email: honming@cuhk.edu.hk
Man-Wah Li; Email: limanwah@cuhk.edu.hk

Keywords:
Histone modification, ChIP-Seq, Transcriptome, Priming, Salt Stress, Soybean, *Glycine max*, Gene network

This article has been accepted for publication and undergone full peer review but has not been through the copyediting, typesetting, pagination and proofreading process which may lead to differences between this version and the Version of Record. Please cite this article as doi: 10.1111/tpj.15652

Abstract

Plants that have experienced certain abiotic stress may gain tolerance to a similar stress in subsequent exposure. This phenomenon, called priming, was observed here in soybean (*Glycine max*) seedlings exposed to salt stress. Time-course transcriptomic profiles revealed distinctively different transcriptional responses in the primed seedlings from those in the non-primed seedlings under high salinity stress, indicating a stress response strategy of repressing unhelpful biotic stress responses and focusing on the promotion of those responses important for salt tolerance. To identify histone marks altered by the priming salinity treatment, a genome-wide profiling of Histone 3 Lysine 4 dimethylation (H3K4me2), Histone 3 Lysine 4 trimethylation (H3K4me3), and Histone 3 Lysine 9 acetylation (H3K9ac) was performed. Our integrative analyses revealed that priming induced drastic alterations in these histone marks, which coordinately modified stress response, ion homeostasis and cell wall modification. Furthermore, transcriptional network analyses unveiled epigenetically modified networks which mediate the strategic downregulation of defense responses. Altering the histone acetylation status using a chemical inhibitor could elicit the priming-like transcriptional responses in non-primed seedlings, confirming the importance of histone marks in forming the priming response.

Introduction

Salinity stress is one of the major abiotic stresses that limits the growth and yield of crops, such as maize, wheat, rice, and soybean, which adversely impact food security (Zorb *et al.*, 2019, Russ *et al.*, 2020). To combat the challenges posed by salinity stress, plants adopted various strategies including the regulation of transcriptional responses and protein activities, maintaining osmotic and ionic balance, and metabolic adjustments (Phang *et al.*, 2008, van Zelm *et al.*, 2020, Yung *et al.*, 2021).

It has been demonstrated that plants can acquire improved tolerance after an initial exposure to abiotic or biotic stresses, which is known as priming (Conrath *et al.*, 2015, Mauch-Mani *et al.*, 2017). Through the priming mechanisms, plants are better prepared for pronounced or timely responses during subsequent encounters of a similar stress (Conrath *et al.*, 2015, Mauch-Mani *et al.*, 2017). By priming plants with a mild salt stress pretreatment, subsequent improvements in salt tolerance were demonstrated through increased photosynthetic parameters, better regulation of K^+/Na^+ ratio, and higher osmotic potential in plants (Umezawa *et al.*, 2000, Shen *et al.*, 2014, Janda *et al.*, 2016, Pandolfi *et al.*, 2016, Pandolfi *et al.*, 2017). The modulation of transcriptional responses is important in regulating a broad range of cellular processes underlying salt stress priming. Recent studies have proposed that epigenetic features such as histone marks may be altered as a consequence of priming, which in turn modify the chromatin status and modulate transcriptional responses during subsequent stress exposure (Zheng *et al.*, 2019, Sun *et al.*, 2020, Fu *et al.*, 2021, Yung *et al.*, 2021). In *Arabidopsis* (*Arabidopsis thaliana*), the increased H3K4me3 levels at *WRKY6*, *WRKY29* and *WRKY53* were followed by higher gene expressions, when the plants were exposed

to the wounding stress directly after the priming pretreatment (Jaskiewicz *et al.*, 2011). In addition, repeated drought stress enhanced H3K4me3 levels at *RESPONSIVE TO DESICCATION 29B* (*RD29B*) and *RESPONSIVE TO ABSCISIC ACID 18* (*RAB18*), leading to the elevated expression of these genes during the subsequent drought stress (Ding *et al.*, 2012). Also, the increase in H3K4me2 and H3K4me3 levels were associated with the enhanced expression of *ASCORBATE PEROXIDASE 2* (*APX2*) and *HEAT SHOCK PROTEINS 22.0* (*HSP22.0*) during the secondary heat stress (Lamke *et al.*, 2016, Liu *et al.*, 2018). After a salt stress pretreatment, an enhanced H3K4me3 level was sustained at *Δ1-PYRROLINE-5-CARBOXYLATE SYNTHETASE 1* (*P5CS1*), which had higher expression, leading to a higher proline content when the plant was subjected to a higher salt concentration than the pretreatment (Feng *et al.*, 2016). While these studies were mainly focused on the assessment of transcriptional memory of the target gene loci, the genome-wide profiles of H3K4me2, H3K4me3, H3K9me2, and H3K27me3 were also generated after a mild salt stress pretreatment in another study in *Arabidopsis* (Sani *et al.*, 2013). The alterations in H3K27me3 levels were concomitant with the changes in the transcriptional responses of *HIGH-AFFINITY K^+ TRANSPORTER 1* (*HKT1*), *PLASMA MEMBRANE INTRINSIC PROTEIN 2E* (*PIP2E*) and two indole-3-acetic acid-amido synthetase-encoding genes, in response to the second salt stress (Sani *et al.*, 2013).

Although the involvement of histone modifications in abiotic stress priming has been reported in several cases in *Arabidopsis*, the roles of histone marks in modulating transcriptional responses in other plant species, especially those economically important crops, remain largely unknown. In soybean, the relationship between histone modifications and transcription has only been assessed in the context of a single salt treatment (Song *et al.*, 2012, Sun *et al.*, 2019). In this study, the effects of pretreatment on improving the tolerance of soybean to high salt stress were examined. By assessing the time-course transcriptomic profile and genome-wide atlases of H3K4me2, H3K4me3, and H3K9ac in leaves and roots of soybean seedlings, we have uncovered the complex processes of transcriptomic and epigenomic reprogramming underlying the phenomenon of salt stress priming. To confirm the roles of histone acetylation in modulating the transcriptional responses of the priming-specific genes, a histone deacetylase inhibitor, Trichostatin A (TSA), was used to pre-treat seedlings to induce changes in histone acetylation without salt stress priming. The transcriptional responses of the priming-specific genes in TSA-treated seedlings were investigated under high salinity stress and compared to those of the salt stress-primed counterparts.

Results

Effects of pretreatment on salt tolerance of soybean seedlings

To investigate the effects of priming on the performance of soybean seedlings in response to salt stress, a mild salt pre-treatment (0.3% NaCl, w/v) was applied to the hydroponic system when the first trifoliates of the seedlings in the treatment group were fully opened. After 6 days, all soybean seedlings were transferred to fresh hydroponic medium containing 0.9% NaCl (w/v) for high salt stress treatment. Upon exposure to high salinity, the non-primed seedlings were severely wilted within 1 h of exposure, in contrast to the primed seedlings which were comparable to the untreated control (Figure 1A). The photosynthetic performances of primed seedlings, in terms of the photosynthetic rate and stomatal conductance, were much less affected by the high salt treatment than those of the non-primed seedlings after 2 d (Figure 1B and C). Three days after high stress treatment, the primed seedlings also maintained a much lower Na^+/K^+ ratio in leaves than the non-primed seedlings. In fact, the Na^+/K^+ ratio in the leaves of primed seedlings was not significantly changed by the high salt treatment at all (Figure 1D). This shows that the mild salt stress pre-treatment had effectively primed soybean seedlings and allowed them to acquire higher tolerance to the subsequent stress. Proline is well-known as an osmolyte which contributes to salt tolerance. The proline contents in both leaves and roots of primed seedlings were significantly lower than those of non-primed seedlings at 3 d after high salinity stress (Figure 1E). This suggests that the enhanced salt tolerance after priming was not caused by proline accumulation. Instead, the lower proline content in primed seedlings may be due to better protection by other factors, reducing the need for substantial osmotic re-balancing in the late phase of salt stress response.

Primed soybean seedlings have distinctly different transcriptional responses under high salinity stress from non-primed seedlings

As sessile organisms, plants adopt several strategies to withstand salt stress. In addition to the physiological adjustments to maintain metabolism and ion homeostasis, the stress signal transduction triggers the mediation of transcriptional responses in the pathways important for salt stress adaptations (Phang *et al.*, 2008, van Zelm *et al.*, 2020, Yung *et al.*, 2021). To investigate the impact of the priming treatment on the transcriptional responses of soybean seedlings during subsequent encounters of high salinity stress, RNA-seq was conducted using the leaves and roots of primed and non-primed seedlings harvested at 0 h, 0.5 h, 1 h, 2 h, 8 h and 24 h from the start of the high salinity stress treatment.

To compare with the transcriptional patterns previously identified in soybean seedlings under salt stress, genes with patterns of differential expression ($p < 0.05$) between primed and non-primed seedlings were obtained (Table S1) (Liu *et al.*, 2019a). The non-primed seedlings displayed a transcriptomic profile in line with our previous findings in soybean seedlings under high salt stress (Liu *et al.*, 2019a), where photosynthetic genes were generally repressed at both early and late stages of the response, as the photosynthetic rate sustained a decrease after stress application. However, a reverse transcriptional pattern

was observed in the primed seedlings. Most of the photosynthetic genes involved in the light and dark reactions showed an upregulation trend in primed seedlings, compared to non-primed ones (Figure S1).

Previously, the carbon catabolic pathways were found to be enhanced in the leaves in response to salt stress (Liu *et al.*, 2019a), whereas in this study, the genes encoding glycolytic GAPDH, one of the rate-limiting enzymes in glycolysis, were repressed in primed seedlings (Figure S2A). In addition, most of the genes involved in the tricarboxylic acid cycle, including those encoding the rate-limiting enzyme citrate synthase, were repressed in the leaves of the primed seedlings (Figure S2B). These results suggest that primed seedlings had a distinctly different response in carbon catabolism and energy production in subsequent stress exposure compared to non-primed ones.

In response to salt stress, the transcriptomic profile of soybean seedlings also indicated the redistribution of nitrogen and carbon resources incorporated in amino acids in leaves, which was important for adaptation to the impaired energy production from photosynthesis (Liu *et al.*, 2019a). In this study, two genes involved in the conversion of branched-chain amino acids and alanine to glutamate were downregulated in the leaves of primed seedlings at the late stage of stress (Figure S2C). Moreover, some genes involved in the catabolism of branched chain amino acids and lysine into organic acids were also repressed at the same stage (Figure S3). The lower requirements in the redistribution of resources suggest that the primed seedlings could maintain better metabolic balance and energy supply under high salt stress than non-primed ones.

For downstream analysis, we further filtered the differentially expressed genes between the primed and non-primed seedlings (DEGs, fold change > 1.5 and q-value < 0.05). In total, we identified 2,693 and 14,449 DEGs in at least one time point in leaves and roots, respectively (Data Set S1). As indicated by the GO enrichment analysis, priming led to alterations in reactive oxygen species (ROS) homeostasis in roots. When the primed seedlings were exposed to subsequent high salinity stress, the GO terms for hydrogen peroxide and ROS metabolic processes were enriched in downregulated DEGs in the roots at 0.5 h and 1 h after stress (Data Set S2). From the results of the Kyoto Encyclopedia of Genes and Genomes (KEGG) enrichment analysis, genes responsible for sugar and amino acid metabolism were differentially regulated in roots after the 6-day pretreatment (0 h), which reflected the different metabolic states between primed and non-primed seedlings (Data Set S3). Upon high salinity treatment, transcriptional changes in metabolic pathways between the two groups of seedlings were prominent at late phases (8 h and 24 h) of high salinity stress (Data Set S3), which is in line with our previous report (Liu et al., 2019a).

Alterations in the expression patterns of gene networks in primed versus non-primed seedlings under high salinity stress

During abiotic stress priming, plants may have potentiated gene expressions in later stress responses (Conrath *et al.*, 2015). To identify the transcriptional networks constituting the distinct transcriptomic responses, weighted gene co-expression network analysis (WGCNA) was performed using the DEGs

between the primed and non-primed seedlings. The DEGs were clustered into 16 and 22 modules in leaves (L-Ms) and roots (R-Ms), respectively (Figure S4, Figure S5, Data Set S4, Data Set S5). Among the upregulated modules, L-M1 includes genes involved in cell wall organization, such as the gene encoding the homologs of regulators of cell wall synthesis, *SND2*. In addition, L-M2 were characterized by the faster transcriptional responses of the homologous genes of *RESPONSIVE TO DESICCATION 29B* (*RD29B*) and *HIGHLY ABA-INDUCED PP2C GENE 3 (HAI3)* at the early stages (0.5 h and 1 h) in primed seedlings. Faster responses of these genes may contribute to faster signaling for a timely modulation of downstream protective mechanisms against high salinity stress in leaves.

On the other hand, we also identified gene modules that were transcriptionally less responsive after priming, which were less frequently reported in other studies (Figure S4). L-M3 and L-M4 were enriched with genes involved in defense responses and plant-pathogen interactions, including 34 WRKY transcription factor genes and 76 disease resistance (R) protein-coding genes. The repression of early-stage defense-responsive genes was also observed in R-M1 (Figure S5). These results suggest that a strategic downregulation of the early defense responses may be involved in salt stress priming. Our findings suggest that the differential transcriptional responses in leaves and roots at early stages of high salinity stress share co-expression modules linked to important pathways involved in stress responses. Also, both potentiated and depleted induction seemed to be important regulatory mechanisms of distinct pathways during salt stress priming.

Priming induces alterations in histone modifications in soybean seedlings

As emerging studies have revealed that epigenetic mechanisms, especially histone modifications, can regulate the expression of key genes controlling stress tolerance, we performed chromatin immunoprecipitation followed by sequencing (ChIP-seq) to identify genome-wide changes in the H3K4me2, H3K4me3, and H3K9ac levels following the priming treatment. The summary of each sequencing library and the correlation between biological replicates are shown in Table S1 and Figure S6. Comparative analyses between primed and non-primed groups showed that the largest difference in both leaves and roots was in the H3K4me3 profile, in which 16,198 and 16,095 differential region-related genes (DRGs, the nearest gene to the differential regions located 2 kb upstream of TSS and/or gene body) were observed in leaves and roots, respectively (Table S2 and Dataset S1). Also, the analysis identified 581 and 391 DRGs with differences in H3K9ac and H3K4me2 in leaves, respectively (Table S2). In roots, 5,066 and 3,415 DRGs were identified with differences in H3K9ac and H3K4me2, respectively (Table S2). These suggest that the priming treatment induced drastic changes in the histone modification profiles in both leaves and roots of soybean seedlings.

The relationships between H3K4me2, H3K4me3, and H3K9ac and transcriptomic profiles

To understand the impacts of priming-induced alterations in histone modification profiles on future encounters with salt stress, we compared the enrichment profiles of H3K4me2, H3K4me3 and H3K9ac to

the transcriptomic data. We first assessed the relationship between the level of histone modification enrichment and the expression of the associated genes. As shown in Figure 2A and 2B, the enrichment levels of H3K4me3 and H3K9ac along genic regions increased with increasing transcript levels (FPKM values) in both leaves and roots of seedlings after the 6-day priming treatment, whereas the H3K4me2 levels and the transcript levels of the related genes were negatively correlated in both tissues of primed seedlings (Figure 2A and B). Also, we confirmed similar relationships between transcript and histone mark enrichment levels in both tissues of non-primed seedlings (Figure S7). Our findings demonstrated that the general roles of H3K4me2 as a repressive mark and those of H3K4me3 and H3K9ac as active marks in relation to transcription are conserved in soybean and other plant species (Wang *et al.*, 2009, Liu *et al.*, 2019b, Huang *et al.*, 2021).

Based on this confirmation, with high-quality data, of a consistent relationship between histone marks and transcriptional alterations, we screened for the DEGs between primed and non-primed seedlings exposed to the subsequent high salinity stress with the change in transcript levels in the same direction as predicted by the associated histone modifications at any time points, and we labeled them DRG-DEGs (Figure 2C). In total, 781 and 4,607 DRG-DEGs were identified in leaves and roots, respectively (Figure 2C). Statistical analysis showed that the DRGs significantly overlapped with the DEGs, except for the genes with increased H3K9ac levels in leaves (Figure 2C). Two cases were selected and visualized in Figure 2D. Next, we analyzed the potential functions of these DRG-DEGs. GO enrichment analyses showed that the GO terms involved in defense response, stress response and signaling were enriched in downregulated DEGs associated with less active marks in leaves (H3K4me3) and roots (H3K4me3 or H3K9ac) of primed seedlings compared to non-primed seedlings (Figure 2E, Data Set S6). Besides, these GO terms were also enriched in the downregulated DEGs with higher levels of repressive mark (H3K4me2) in roots (Figure 2E, Data Set S6).

On the other hand, the terms related to cell wall components were enriched in downregulated DEGs marked by changes in H3K4me3 levels in leaves and upregulated DEGs with changes in H3K4me3 or H3K9ac levels in roots (Figure 2E, Data Set S6). These suggest that priming-induced alterations in histone modifications were tightly linked to the transcriptional changes between primed and non-primed seedlings in the cellular processes involved in abiotic stress responses. Besides, the enrichment of terms related to cell cycle, DNA and RNA processes in the upregulated DEGs marked by increased H3K4me3 level in roots implied that the cell cycle was less affected by high salinity stress in primed seedlings (Figure 2E, Data Set S6).

Changes in histone modifications are associated with altered transcriptional responses of several components of dehydration-responsive pathways and ion homeostasis

As the regulators of stress signaling were consistently identified in the differential expression modules in both tissues, we hypothesized that the priming-induced alterations in histone marks were also involved in modifying chromatin status at the DEGs encoding components of dehydration-responsive pathways and

ion homeostasis. Abscisic acid (ABA) signaling is well known to mediate responses to the osmotic components of salt stress (Umezawa *et al.*, 2010, Yoshida *et al.*, 2014). ABA is perceived by the PYL/PYR/RCAR receptors (Umezawa *et al.*, 2010). According to our data, the less active chromatin status of *PYL4 (Glyma.01G124700)* in the leaf (lower H3K4me3 level) was consistent with the downregulation of the gene at 1 h after high salinity stress (Figure 3A). At the same time, the upregulation of *PYL4* and *PYL6* in the root corresponded to the elevated levels of activating histone marks, especially at 0.5 h after high salt treatment (Figure 4A).

Protein phosphatase 2Cs (PP2Cs) negatively regulates ABA signaling by dephosphorylating SNF1-Related Protein Kinases type 2 (SnRK2s) and are also involved in fine-tuning the signaling pathway (Wang *et al.*, 2019). In this study, the more active chromatin status, featured by the increase in the active mark H3K4me3 and the decrease in the repressive mark H3K4me2, was linked to the upregulation of *HAI3*, which encodes PP2Cs, in both tissues of the primed seedlings at the early stage of high salt stress (Figure 3A, Figure 4A). Also, differential histone modifications and gene expressions were observed in a *SnRK2.6* gene *(Glyma.01G204200)* in leaves and another *(Glyma.07G178600)* in roots after stress (Figure 3A, Figure 4A). These findings suggested that several layers of ABA signaling were differentially regulated in primed seedlings.

The responses to osmotic and salt stress can also be mediated through an ABA-independent signaling pathway, in which DREB transcription factors are responsible for transcriptional regulation (Yoshida *et al.*, 2014). Here in primed seedlings, the genes in the *DREB1* family were downregulated in primed seedlings compared to non-primed seedlings after high salt stress, including a gene modified by the less active chromatin status in roots (Figure 4B). As DREB1 transcription factors are key regulators of cold tolerance (Ito *et al.*, 2006), these results also suggested that unnecessary signaling pathways were downregulated by salt priming. Furthermore, a gene related to the TINY transcription factor in the DREBA-4 subfamily from *Arabidopsis* was modified by more active histone marks and upregulated in the leaves of primed seedlings at the early stage (0.5 h) (Figure 3B), whereas in roots, two *TINY*-related genes were associated with more active histone marks and were upregulated at 8 h after stress (Figure 4B). In addition, genes downstream of the ABA-dependent and ABA-independent pathways, including those encoding RD22 or RD29B that are crucial for salt tolerance, were upregulated in the leaves of primed seedlings under high salinity stress (Figure 3A and 3B), suggesting that the output of the alterations in upstream transcriptional responses could facilitate salt tolerance downstream.

As the accumulation of sodium and chloride ions imposes toxic effects on plant metabolism and physiological processes, ion homeostasis mediated by transporters and channels is important for conferring salt tolerance. From the transcriptomic analysis, differential expression was observed in the members of the *CATION/H^+ EXCHANGER* (*CHX*), *HIGH-AFFINITY K^+ TRANSPORTER* (*HKT*) and *NA^+/H^+ ANTIPORTER* (*NHX*) families (Figure 3C, Figure 4C, Figure S8). The lower H3K9ac level was consistent with the downregulation of *GmCHX20a* in the leaves of primed seedlings (Figure 3C). In roots, the

upregulation of *GmCHX1* was also in line with the increased H3K4me3 level in primed seedlings (Figure 4C). However, differential histone marks were not observed in the genes encoding HKT1, a transporter that removes sodium ions from the transpiration stream in *Arabidopsis* (Davenport *et al.*, 2007) (Figure S8).

The transcriptomic data also revealed differential regulation of the chloride channel (CLC) family, which is responsible for the sequestration of chloride ions into vacuoles (Teakle and Tyerman, 2010, Nguyen *et al.*, 2016). Differential histone modifications were linked to the lower expression of a *CLCb* homolog in leaves (Figure 3C), and the higher expression of *GmCLC1* in roots of primed seedlings (Figure 4C). The alterations in the histone modifications and expressions of *CLCs* in both directions suggested the complicated regulation of chloride ion homeostasis during salt stress priming.

The early-stage differential transcriptional networks were modified by the priming-altered histone modifications

Since concurrent priming-induced alterations in histone modifications and gene expressions were observed in transcription factor (TF) genes, as indicated by the results of the GO enrichment analysis and investigation on stress-responsive pathways, we hypothesized that these DRG-DEGs could potentially lead to the differential regulation of their downstream targets, thus broadening the initial effects of priming. Hence, we analyzed the distributions of transcription factor binding motifs at the promoter regions of all DEGs between the primed and non-primed seedlings across all time points. The consensus binding motifs for the ABA-responsive element (ABRE), dehydration-responsive element (DRE), GCC-box, and W-box TFs were selected for this analysis. In leaves, the ABRE, DRE and W-box motifs were significantly enriched in both the upregulated and downregulated DEGs across most of the time points after stress (Figure 5A). In contrast, the GCC-box was significantly enriched only in downregulated DEGs at 0 h and 0.5 h, although it was also enriched in both the upregulated and downregulated DEGs at the late stage (8 h and 24 h) (Figure 5A). In roots, the DRE element was significantly enriched in upregulated DEGs in the primed seedlings before the onset of high salinity stress treatment (Figure S9). All four motifs were enriched in the DEGs throughout the entire duration of the high salinity stress (Figure S9).

As substantial transcriptional regulation of stress responsive pathways was observed between the primed and non-primed seedlings, the DEGs were further analyzed to identify potential TF networks involved at the early stages of salt stress. In total, 117 and 194 putative transcriptional networks were identified from the DEGs at 0.5 h or 1 h in leaves and roots, respectively. Among the 7 networks with downregulated hub TF genes in leaves, 3 of the *WRKY*-centered networks were modified by lower H3K4me3 levels (Table S3). The putative networks anchored by these 3 *WRKY*s included 108 target genes, of which 29 were also marked by differential histone marks for a less active chromatin status (Figure 5B, Table S4). Also, the genes related to defense responses were enriched in this integrative priming-downregulated network. This suggested that salt priming-altered histone modifications could modulate the transcription of WRKY-encoding genes and their downstream networks implicated in defense responses. In addition, 22 out of 29 DRG-DEGs in the *WRKY*-centered networks were found to be members of L-M3 or L-M4, which were

identified in the WGCNA analysis and linked to defense response (Table S4).

Trichostatin A pre-treatment enhanced photosynthetic performance and transcriptional responses of selected genes with differential H3K9ac levels in non-primed seedlings exposed to high salinity stress

To confirm the role of altered H3K9ac levels in regulating transcriptional responses upon salt stress priming, we pretreated non-primed soybean seedlings for six days using the histone deacetylase inhibitor, Trichostatin A (TSA), before exposing them to high salt stress. Under high salinity stress, the photosynthetic rate in the TSA-treated seedlings was higher than that in the non-primed, non-TSA-treated seedlings, although it was lower than that in the primed seedlings (Figure 6A). This indicates that TSA-treated seedlings have enhanced photosynthetic performance compared to the non-primed seedlings when exposed to high salinity stress. Next, we questioned if TSA treatment could alter the local H3K9ac level at priming-specific genes. As indicated by Figure 6B, TSA-treated seedlings displayed higher H3K9ac levels at the genes which encode *GmCLC1*, *ARF16-*, *PP2C68-* and *SCR-related* in roots, than those in the non-primed seedlings. A higher H3K18ac level was also observed at *PP2C68-related* in TSA-treated seedlings when compared to the non-primed seedlings, although priming by mild salt stress led to higher H3K18ac levels at all the four genes (Figure S10). Moreover, the expression levels of these genes were higher in the TSA-treated seedlings than those in the non-primed seedlings at 0.5 h after high salinity stress treatment (Figure 6C). These indicated that increases in the histone acetylation level could lead to enhanced transcriptional response of priming-induced genes.

Discussion

Priming enhanced salt tolerance of soybean seedlings

Priming has been documented as an adaptive process responsible for enhancing stress tolerance in plants, in which the strategic regulation of gene expressions was initiated by environmental stimuli to prepare for more effective responses upon subsequent stress challenge (Conrath *et al.*, 2015, Mauch-Mani *et al.*, 2017). In this study, we demonstrated that priming by mild salt stress could enhance salt tolerance in soybean, as indicated by the higher photosynthetic assimilation rate and more stable ion homeostasis in primed seedlings compared to non-primed seedlings (Figure 1A-1D).

Proline accumulation is one of the signatures of salt stress priming in *Arabidopsis* (Feng *et al.*, 2016). However, the proline content in primed soybean seedlings was lower than that in non-primed seedlings under salt stress (Figure 1E). This suggested that salt stress priming in soybean did not involve proline accumulation. Indeed, the proline contents under salt stress were poorly correlated with salt tolerance in different soybean germplasms (Phang *et al.*, 2008). This discrepancy implies that the priming mechanisms in soybean may be distinct from those in *Arabidopsis* and raises the need to investigate the underlying

pathways in soybean independently from the *Arabidopsis* model.

Priming directed the strategic regulation of both early- and late-stage transcriptional responses to high salinity stress

By comparing the time-course transcriptomic profiles, we identified drastic changes in the transcriptional responses between primed and non-primed seedlings under salt stress. Overall, the primed seedlings displayed the reverse patterns to non-primed seedlings in gene expressions in multiple pathways, including photosynthesis, carbon catabolism, and the redistribution of carbon and nitrogen resources. Notably, these pathways were also identified in our previous study to be the major ones that experienced differential regulation (Liu *et al.*, 2019a), suggesting that priming triggers the establishment of a transcriptomic profile distinct from the common salt stress response.

Using the DEGs identified between primed and non-primed seedlings ($q < 0.05$ and fold change > 1.5), WGCNA revealed that at the early stage (0.5 h and 1 h) of high salinity stress, there were higher induction of modules containing the regulators of osmotic stress responses (L-M1 and L-M2) and repression of those related to defense responses (L-M3, L-M4 and R-M1) in primed seedlings (Figure S4, Figure S5, Data Set S4, Data Set S5). In plants, the oxidative burst at the early stage was important in triggering defense responses mediated by salicylic acid (SA) signaling, in which NON-EXPRESSOR OF PR GENES 1 (NPR1) coactivates downstream gene expressions (Wojtaszek, 1997, Herrera-Vasquez *et al.*, 2015). The decreased induction of modules containing defense genes (e.g. R-M1) in roots may be linked to the downregulation of hydrogen peroxide metabolic processes, as indicated by the GO enrichment analysis, at the early stage (0.5 h and 1 h) of high salinity stress (Figure S5, Data Set S2). Our findings suggest that the early transcriptional responses were strategically regulated during salt stress priming, to enable rapid gene inductions which bring on early osmotic stress responses in leaves for the timely activation of protective mechanisms. At the same time, repressing defense responses that might otherwise make unnecessary demands on cellular mechanics could enable a focused osmotic stress response.

Besides, the upregulation of modules containing genes involved in cell wall modification through priming (L-M1) may expedite cell wall adjustments in primed seedlings during subsequent salt exposure (Figure S4, Data Set S4). Alterations in cell wall extensibility were proposed to influence cellular osmotic balance and tolerance (Cho *et al.*, 2006, Moore *et al.*, 2008, Lu *et al.*, 2013, Tenhaken, 2015). Moreover, the ectopic expression of *GmRD22* led to increased lignin content and salt and osmotic stress tolerance (Wang *et al.*, 2012). Also, the differential expression of cell wall modification genes at the later stage of stress may be important in growth recovery (Tenhaken, 2015, Rui and Dinneny, 2020). Our study demonstrates that the extensive transcriptional regulation of cell wall modification may contribute to salt stress priming.

Compared to the early response, the late phase (8 h and 24 h) was featured by alterations in a wider range of metabolic pathways, including those related to amino acid, fatty acid, and sugar metabolism (Data Set S3). Massive changes in carbon and nitrogen metabolism are implicated in compensating for the reduced

energy production from photosynthesis when under salt stress (Ji *et al.*, 2016, Liu *et al.*, 2019a). The observation that a higher proportion of these pathways was downregulated may reflect better stress adaptation in primed seedlings.

The global H3K4me2, H3K4me3 and H3K9ac profiles were tightly associated with the transcriptomic program

During priming, alterations in histone marks may act as a record of transcriptional activities during a previous stress and facilitate gene expressions in the subsequent stress (Conrath *et al.*, 2015, Mauch-Mani *et al.*, 2017). Although priming treatment was reported to trigger changes in histone marks at selected stress marker genes (Ding *et al.*, 2012, Feng *et al.*, 2016, Lamke *et al.*, 2016), investigations into the comprehensive profiles of histone marks at the genomic level are scarce (Sani *et al.*, 2013). In this study, the strong correlation between the enrichment levels of H3K4me2, H3K4me3 and H3K9ac with transcription levels was observed (Figure 3, Figure S7), supporting that these histone marks are highly integrated with the transcriptional dynamics. The analysis revealed the role of H3K4me2 as a repressive mark and those of H3K4me3 and H3K9ac as active marks in relation to transcription in soybean.

It was observed that changes in H3K4me3 were linked to a higher number of DRG and DRG-DEGs than those in H3K4me2 and H3K9ac in both roots and leaves, suggesting a more significant role played by H3K4me3 in modulating transcriptional responses during salt priming. Nevertheless, our analyses of the histone modification and transcriptomic profiles showed that the priming-induced changes in H3K4me2, H3K4me3 or H3K9ac were closely related to the altered gene transcription involved in a wide range of processes in roots, including cell wall modification, stress signaling and transcriptional regulation (Figure 2E, Data Set S6). This demonstrates the roles of histone marks in modifying a diversified portfolio of cellular processes during salt stress priming. Recently, the histone acetyltransferase GCN5 was found to positively regulate cell wall formation and salt tolerance in *Arabidopsis* (Zheng et al., 2019). Our study demonstrated that the transcriptional modulation of genes related to cell wall modification by H3K4 methylation may also be important in salt stress priming in soybean.

Priming-specific histone marks modified gene expressions to modulate osmotic stress responses and ion homeostasis

Our integrative data revealed that the priming-induced alterations in histone marks coincided with altered transcriptional responses in the major pathways, including those responsible for osmotic stress response and ion homeostasis (Figure 3, Figure 4, Figure S8). However, unlike previous reports on *Arabidopsis*, we did not observe altered histone marks at the soybean homologs of *RD29B*, *P5CS1,* and *HKT1* (Ding *et al.*, 2012, Sani *et al.*, 2013, Feng *et al.*, 2016). This uncovers a distinction between the epigenetic mechanism in soybean and that in *Arabidopsis* during abiotic stress priming. In soybean, the priming-induced alterations in histone modifications corresponded to the differential expressions in gene members from several layers of the ABA-dependent pathway (Figure 3A, Figure 4A). In addition, the *TINY-related* genes were

upregulated at the early and late stages in the leaves and roots of primed seedlings, respectively (Figure 3B, Figure 4B). Recently, the *Arabidopsis* TINY, a member of the DREBA-4 subfamily, was demonstrated to activate drought-responsive genes and repress brassinosteroid-inducible genes (Xie *et al.*, 2019). Therefore, the upregulation of *TINY-related* genes in the primed soybean seedlings may represent a mechanism to fine-tune the balance between osmotic stress tolerance and plant growth. Moreover, the genes encoding key ion transporters and channels, including GmCHX1 and GmCLC1 (Guan *et al.*, 2014, Qi *et al.*, 2014, Wei *et al.*, 2016, Jia *et al.*, 2021), were differentially modified by histone marks and were differentially expressed in the direction that conferred salt tolerance in roots (Figure 4C), while the gene encoding GmCHX20a was differentially modified and expressed in leaves (Figure 3C). These supported the role of histone modifications in determining the degree of salt tolerance.

The repression of defense response by salt stress priming was potentially mediated by the loss of active histone marks

As shown by the results of the WGCNA, a reduction in the inducibility of defense-responsive genes (e.g. L-M3, L-M4 and R-M1) was observed in primed seedlings (Figure S4, Figure S5, Data Set S4, Data Set S5). At the same time, the W-box consensus motif was enriched in the promoters of downregulated DEGs in primed seedlings (Figure 5A). Together these suggested that the upstream alterations in the expression of WRKY transcription factors, which regulate defense response, could potentially mediate the downregulation of entire gene networks. Consistent with this prediction, three downregulated hub genes encoding WRKYs were modified by reduced levels of active histone marks and had reduced expressions in primed seedlings (Figure 5B), and their associated gene networks were enriched with genes involved in defense responses (Table S4). In addition, a large proportion of members of the WRKY-mediated networks were included in L-M3 and L-M4, supporting that the epigenetically modified networks also participated in the modulation of the defense-related co-expression modules (Table S4). This information supported the hypothesis that histone modifications could modulate the downregulation of WRKY-encoding genes, leading to further repression of defense response networks during salt stress priming. Recently, the involvement of histone modifications in WRKY-mediated networks was also reported in soybean symbiosis with rhizobia (Wang *et al.*, 2020). Together, our studies shed light on the epigenetic mechanisms that facilitate the repression of irrelevant or non-strategic gene networks in order to channel the plant's energy budget towards cellular processes that are beneficial for plant fitness when necessary.

Manipulating H3K9ac levels could alter transcriptional responses under high salinity stress

Although histone modifications have been linked to the expression of priming-specific genes (Ding *et al.*, 2012, Sani *et al.*, 2013, Feng *et al.*, 2016, Friedrich *et al.*, 2021), the information on their regulatory role in the early stress responses is still limited (Yamaguchi *et al.*, 2021). In this study, we tested the effects of altered histone modification on transcriptional response by pretreating seedlings with a histone deacetylase inhibitor, Trichostatin A (TSA). Under high salinity stress, the expression of three homologs of *HISTONE DEACETYLASE 2C (HD2C)* were upregulated in the primed seedlings, suggesting the involvement of

histone deacetylation in salt priming response (Figure S11). Application of TSA was shown to enhance salinity stress tolerance in *Arabidopsis* seedlings (Ueda *et al.*, 2017), whereas in peanut, the TSA treatment led to changes in the expression pattern of *AhDREB1* (Zheng *et al.*, 2019). In this study, it was found that the TSA pretreatment promoted the photosynthetic performance of non-primed seedlings in response to salt stress (Figure 6A). By maintaining the H3K9ac level at the priming-specific genes, including *GmCLC1*, *ARF16*-, *PP2C68*- and *SCR-related* using TSA (Figure 6B), the transcriptional response of these genes could be enhanced at the early stage of high salinity stress (Figure 6C). Although the involvement of H3K18ac in salt priming was also suggested by the differential enrichment at the selected genes in primed seedlings compared to non-primed seedlings, the TSA pretreatment only led to a higher H3K18ac level at *PP2C68-related* (Figure S10), suggesting that the deacetylation processes of H3K9 and H3K18 may involve different regulators. The TSA pretreatment mimicked the increased H3K9ac levels after priming, and the results from this experiment further supported that histone acetylation such as H3K9ac played a key role in modulating priming-specific transcriptional responses to enhance soybean tolerance to salt stress.

Experimental procedures

Plant materials and growth conditions

In a greenhouse, soybean (*Glycine max*) cultivar C08 (variety name: Union, salt-sensitive) seeds were germinated in vermiculite and transferred to a hydroponic system containing half-strength Hoagland's solution when the primary leaves were fully opened (Hoagland and Arnon, 1950). The seedlings were grown at an ambient temperature of 25-28°C under a 12 h/12 h light-dark cycle with supplemental lighting. When the first trifoliates were fully opened, the seedlings were transferred to half-strength Hoagland's solution containing 0.3% (w/v) NaCl for the mild stress pretreatment (priming of seedlings). The non-primed seedlings were transferred to fresh half-strength Hoagland's solution without NaCl as control. For the Trichostatin A (TSA) pretreatment, the seedlings were transferred to half-strength Hoagland's solution containing 1 μM TSA. After a 6-day pretreatment, seedlings from all treatment and control groups were transferred to half-strength Hoagland's solution containing 0.9% (w/v) NaCl for high salinity stress treatment.

Physiological measurements for the evaluation of salt tolerance

Photosynthesis rate and stomatal conductance of the first trifoliates of soybean seedlings were measured with the LI-6400XT portable photosynthesis system (LI-COR; Lincoln, Nebraska, USA) after the 6-day priming treatment and at 0.5 h, 2 h, and 48 h under high salinity stress. Determination of Na^+ and K^+ contents of the first trifoliates was performed as described previously (Qi *et al.*, 2014). Data were analyzed using the Statistical Package for Social Sciences version 27. One-way analysis of variance (ANOVA) followed by Tukey's post hoc test was used to compare the values obtained from different sample groups.

Measurements of proline content

To measure the proline content, the first trifoliates and roots of soybean seedlings were harvested at 0 d and 3 d after the high salinity stress treatment. After measuring the fresh weight, the samples were immediately frozen in liquid nitrogen and stored at -80°C before being used for extraction. Determination of proline content was performed as described previously with minor modifications (Bates *et al.*, 1973). Around 1 g of first trifoliates or 2 g of roots was ground to a fine powder in liquid nitrogen using mortar and pestle, and homogenized in 6 mL of 3% sulfosalicylic acid. The homogenate was then filtered through Whatman #1 filter paper. In a glass test tube, 2 mL of the filtrate was mixed with the same volume of acid ninhydrin and glacial acetic acid. The reaction mixture was placed in a water bath at 100°C for 1 h. After cooling on ice, 4 mL of toluene was added to the mixture, which was then mixed by vortexing. The absorbance of the aqueous solution at 520 nm was measured using the Synergy H1 Hybrid Reader (BioTek, USA). The proline concentration was determined from a standard curve and expressed on a fresh weight basis (Bates *et al.*, 1973).

Chromatin immunoprecipitation sequencing (ChIP-seq) analysis

After the 6-day priming treatment, 1 g per sample of first trifoliates and roots were harvested and crosslinked using 1% formaldehyde and stored at -80°C until use. Nuclei isolation and lysis were performed as previously described (Wang *et al.*, 2020). The nucleic lysate from the first trifoliates and roots was sonicated with 17 and 21 cycles (30 s on / 30 s off), respectively, using the 'High Power' mode in the Bioruptor UCD-200 (Diagenode, Belgium). After preclearing the sonicated chromatin, the ChIP reactions were performed using 4 µg anti-H3K4me2 (ab32356, Abcam, UK), anti-H3K4me3 (07-473, MilliporeSigma, USA), anti-H3K9ac (ab10812, Abcam, UK), or anti-H3K18ac (ab1191, Abcam, UK) antibodies as previously described (Wang *et al.*, 2020). After washing and elution, reverse-crosslinking was performed with 200 mM NaCl at 65°C for 6 h, and the ChIP'ed DNA was purified with DNA Clean & Concentrator (Zymo Research, USA; Wang *et al*., 2020).

ChIP'ed DNA libraries were prepared from two independent experiments and sequenced on the Illumina HiSeq 2500 (Macrogen, Korea) or NovaSeq 6000 platform (Novogene, China). Raw reads were trimmed by TrimGalore (https://github.com/FelixKrueger/TrimGalore) to filter out low-quality and adaptor sequences. Then, the clean reads were aligned to the soybean reference genome (*Glycine max Wm82.a4.v1*) (Schmutz *et al.*, 2010) by bowtie2 (Langmead and Salzberg, 2012) with default parameters. The BEDTools suite (Quinlan and Hall, 2010) was then used to convert uniquely aligned reads to bed format which was passed to diffReps (Shen *et al.*, 2013) for the calculation of significantly enriched regions. The q-value of ≤ 0.05 and fold change > 1.2 were used as the cut-off for the calculation of significance between the primed and non-primed seedlings. All metaplots of histone modifications were plotted by deepTools (Ramirez *et al.*, 2014). All sequencing data in this project were visualized in JBrowse (Buels *et al.*, 2016; https://datahub.wildsoydb.org).

RNA-seq analysis

The first trifoliates and roots were harvested at 0 h, 0.5 h, 1 h, 2 h, 8 h, and 24 h under high salinity stress treatment, immediately frozen in liquid nitrogen and stored at -80°C until use. Total RNA was extracted using TRIzol reagent (Thermo Fisher, USA) according to the manufacturer's protocol. RNA libraries from three independent experiments were sequenced with the Illumina NovaSeq 6000 platform (BGI, China). The low-quality and adaptor sequences of raw reads were trimmed by TrimGalore (https://github.com/FelixKrueger/TrimGalore). The hisat2 program (Kim *et al.*, 2015) was used to align the trimmed reads to the same reference genome as in the ChIP-seq analysis. All the concordantly aligned pairs were extracted with samtools (Li *et al.*, 2009) and used to calculate the counts or fragments per kilobase of transcript per million mapped reads (FPKM) value by StringTie (Pertea *et al.*, 2016). The counts of genes were used for differential expression analysis (for comparison of transcriptional patterns with previous results: p-value < 0.05; for downstream DEGs analysis: q-value < 0.05 and fold change > 1.5) by DEseq2 (Love *et al.*, 2014). The heatmaps of selected DEGs were plotted by pheatmap (https://CRAN.R-project.org/package=pheatmap).

Weighted gene co-expression network analysis (WGCNA)

To identify the patterns of early- and late-stage transcriptional responses between primed and non-primed seedlings, genes that were differentially expressed in at least one time point (q-value < 0.05, fold change > 1.5 and max FPKM □1) in the same tissue were combined. The $\log_2$(FPKM+1) values of the DEGs were used in weighted gene co-expression network analysis by the WGCNA R package (Langfelder and Horvath, 2008). The soft threshold power of 18, the minimum module size of 10, and the cut height of 0.25 were used as the parameters for constructing the weighted gene co-expression network. The clustered modules were then visualized by ggplot2 (Wickham, 2009).

Gene Ontology (GO) and Kyoto Encyclopedia of Genes and Genomes (KEGG) pathway enrichment analyses

Gene Ontology (GO) enrichment analysis was performed using agriGO v2.0 (Tian *et al.*, 2017). The enrichment analysis was performed using the Chi-square test and Benjamini-Yekutieli False Discovery Rate. Kyoto Encyclopedia of Genes and Genomes (KEGG) pathway enrichment analysis was performed on selected genes by KOBAS3.0 (Xie *et al.*, 2011) with default parameters. GO and KEGG terms with corrected p-value < 0.05 were considered significantly enriched.

Transcription factor (TF) motif and target enrichment analyses

The counts of selected TF motifs, including AREB, DREB, GCC-box and W-box (Fujimoto *et al.*, 2000, Hattori *et al.*, 2002, Xu *et al.*, 2006, Mizoi *et al.*, 2013) at the promoters of time-point DEGs and all the genes in the reference genome were calculated. The hypergeometric distribution test was performed to test whether the selected motif was enriched in the DEG datasets (Lee and Bailey-Serres, 2019). The bar graphs of motif enrichment results were plotted by ggplot2 (Wickham, 2009). The TF target enrichment

analysis was conducted and visualized as described previously (Wang *et al.*, 2020) with the cut-off at p-value < 0.05. The DEGs at 0.5 h and 1 h in the same direction were merged as the inquiry gene set.

RT-qPCR and ChIP-qPCR analyses

After total RNA extraction, DNase I treatment was performed following manufacturer's instructions (Invitrogen, USA). The resulting RNA was then diluted 10-fold with RNase-free water to 10 ng/μL. Quantitative reverse transcription PCR (RT-qPCR) was performed using the One-Step TB Green PrimeScript RT-PCR Kit II (Takara Bio, USA) with 2.25 μL of diluted RNA as template in each 15 μL reaction. The reactions were run on the CFX384 Touch Real-Time PCR Detection System (Bio-Rad, USA). The thermal cycler was programmed with an initial 5 min at 42°C and 3 min at 95°C, followed by 40 cycles of 10 s at 95°C and 30 s at 58°C. Relative gene expression was calculated using the $2^{-\Delta\Delta CT}$ method (Livak and Schmittgen, 2001). *Bic-C2* and *F-box protein2* were used as the reference genes (Wang *et al.*, 2020).

For ChIP-qPCR, the ChIP'ed DNA was diluted 50-fold and the INPUT control was diluted 100-fold. 1.5 μL of diluted DNA was added to a reaction mixture containing 0.4 μL forward primer (10 μM), 0.4 μL reverse primer (10 μM), 5 μL iQ SYBR Green Supermix (Bio-Rad, USA) and 2.7 μL Milli-Q water. The reactions were run on the CFX384 Touch Real-Time PCR Detection System (Bio-Rad, USA). The thermal cycler was programmed with an initial 3 min at 95°C, followed by 40 cycles of 10 s at 95°C and 30 s at 58°C. The H3K9ac and H3K18ac enrichment was expressed as %INPUT based on Ct values (Wang *et al.*, 2020). The primers used in the qPCR reactions were listed in Table S5.

Data Availability

All the raw sequences generated in this study were deposited at the NCBI under the accession number PRJNA753632.

Acknowledgments

This work was supported by grants from the Hong Kong Research Grants Council Area of Excellence Scheme (AoE/M-403/16) and Lo Kwee-Seong Biomedical Research Fund to H.-M.L. W.-S.Y. was supported by the Dr. Walter Szeto Memorial Scholarship. M.-K.H. was supported by the Impact Postdoctoral Fellowship Scheme of the Chinese University of Hong Kong. We would like to thank Ms. Jee Yan Chu for copy-editing this manuscript and Dr. Zhixia Xiao for his comments on this manuscript. Any opinions, findings, conclusions or recommendations expressed in this publication do not reflect the views of the Government of the Hong Kong Special Administrative Region or the Innovation and Technology Commission. The authors declare that they have no conflict of interest.

Author Contributions

H.-M.L., M.-W. L., W.-S.Y., and Q.W. designed the research. W.-S.Y., Q.W., M.H., M.-W.L., F.-L.W, A. L., M.-S.N., K.-P.L., and C.-C.S. performed the experiments. Q.W. and W.-S.Y. performed bioinformatics analyses. W.-S.Y. and Q.W. interpreted the data. W.-S.Y., Q.W., and H.-M.L. co-wrote the manuscript. H.-M.L. and M.-W. L. supervised the research.

Supporting Information

Figure S1. Heatmaps showing the genes with patterns of differential expression in the photosynthetic pathways in leaves.

Figure S2. Heatmaps showing the genes with patterns of differential expression of glycolysis and tricarboxylic acid cycle pathways in leaves.

Figure S3. Heatmaps showing the genes with patterns of differential expression of lysine and branched-chain amino acid degradation pathways in leaves.

Figure S4. Overall expression patterns of remaining modules identified by weighted gene co-expression network analysis (WGCNA) in leaves.

Figure S5. Overall expression patterns of remaining modules identified by weighted gene co-expression network analysis (WGCNA) in roots.

Figure S6. Pearson correlation analyses of ChIP-seq libraries.

Figure S7. The association between histone modifications and gene expressions in non-primed seedlings.

Figure S8. Heatmaps showing the differentially expressed genes (DEGs) of the HKT1 and NHX families in roots.

Figure S9. Transcriptional modulation of differentially expressed genes (DEGs) by different transcription factor (TF) families in roots.

Figure S10. The enrichment levels of H3K18ac at several priming-related genes.

Figure S11. Heatmaps showing the differentially expressed *HD2C* homologs in roots.

Table S1. Summary of RNA-seq and ChIP-seq libraries.

Table S2. Number of genes with differential histone modifications (DRGs) identified in the leaves and roots of primed seedlings compared to non-primed seedlings.

Table S3. List of transcription factors (TFs) whose putative targets were enriched among downregulated genes in the leaves of primed seedlings compared to non-primed seedlings at 0.5 h or 1 h after high

salinity stress.

Table S4. List of downregulated genes in leaves which are putative targets of WRKY transcription factors.

Table S5. Primers used in this study.

Data Set S1. Transcript levels, differential expression and differential histone modification statuses of all annotated genes in the soybean genome after salt stress priming.

Data Set S2. Gene ontology (GO) enrichment analysis results of differentially expressed genes (DEGs).

Data Set S3. Kyoto Encyclopedia of Genes and Genomes (KEGG) enrichment analysis results of DEGs.

Data Set S4. DEGs sorted according to the selected weighted gene co-expression network analysis (WGCNA) modules in leaves.

Data Set S5. DEGs sorted according to the selected weighted gene co-expression network analysis (WGCNA) modules in roots.

Data Set S6. Gene ontology (GO) enrichment analysis results of DRG-DEGs.

References

Bates, L.S., Waldren, R.P. and Teare, I.D. (1973) Rapid Determination of Free Proline for Water-Stress Studies. *Plant Soil*, **39**, 205-207.

Buels, R., Yao, E., Diesh, C.M., Hayes, R.D., Munoz-Torres, M., Helt, G., Goodstein, D.M., Elsik, C.G., Lewis, S.E., Stein, L. and Holmes, I.H. (2016) JBrowse: a dynamic web platform for genome visualization and analysis. *Genome Biol*, **17**.

Cho, S.K., Kim, J.E., Park, J.A., Eom, T.J. and Kim, W.T. (2006) Constitutive expression of abiotic stress-inducible hot pepper CaXTH3, which encodes a xyloglucan endotransglucosylase/hydrolase homolog, improves drought and salt tolerance in transgenic Arabidopsis plants. *Febs Lett*, **580**, 3136-3144.

Conrath, U., Beckers, G.J.M., Langenbach, C.J.G. and Jaskiewicz, M.R. (2015) Priming for Enhanced Defense. *Annu Rev Phytopathol*, **53**, 97-119.

Davenport, R.J., Munoz-Mayor, A., Jha, D., Essah, P.A., Rus, A. and Tester, M. (2007) The Na+ transporter AtHKT1;1 controls retrieval of Na+ from the xylem in Arabidopsis. *Plant Cell Environ*, **30**, 497-507.

Ding, Y., Fromm, M. and Avramova, Z. (2012) Multiple exposures to drought 'train' transcriptional responses in Arabidopsis. *Nat Commun*, **3**.

Feng, X.J., Li, J.R., Qi, S.L., Lin, Q.F., Jin, J.B. and Hua, X.J. (2016) Light affects salt stress-

induced transcriptional memory of P5CS1 in Arabidopsis. *P Natl Acad Sci USA*, **113**, E8335-E8343.

Friedrich, T., Oberkofler, V., Trindade, I., Altmann, S., Brzezinka, K., Lamke, J., Gorka, M., Kappel, C., Sokolowska, E., Skirycz, A., Graf, A. and Baurle, I. (2021) Heteromeric HSFA2/HSFA3 complexes drive transcriptional memory after heat stress in Arabidopsis. *Nat Commun*, **12**.

Fu, Z.W., Li, J.H., Feng, Y.R., Yuan, X. and Lu, Y.T. (2021) The metabolite methylglyoxal-mediated gene expression is associated with histone methylglyoxalation. *Nucleic Acids Res*, **49**, 1886-1899.

Fujimoto, S.Y., Ohta, M., Usui, A., Shinshi, H. and Ohme-Takagi, M. (2000) Arabidopsis ethylene-responsive element binding factors act as transcriptional activators or repressors of GCC box-mediated gene expression. *Plant Cell*, **12**, 393-404.

Guan, R.X., Qu, Y., Guo, Y., Yu, L.L., Liu, Y., Jiang, J.H., Chen, J.G., Ren, Y.L., Liu, G.Y., Tian, L., Jin, L.G., Liu, Z.X., Hong, H.L., Chang, R.Z., Gilliham, M. and Qiu, L.J. (2014) Salinity tolerance in soybean is modulated by natural variation in GmSALT3. *Plant J*, **80**, 937-950.

Hattori, T., Totsuka, M., Hobo, T., Kagaya, Y. and Yamamoto-Toyoda, A. (2002) Experimentally determined sequence requirement of ACGT-containing abscisic acid response element. *Plant Cell Physiol*, **43**, 136-140.

Herrera-Vasquez, A., Salinas, P. and Holuigue, L. (2015) Salicylic acid and reactive oxygen species interplay in the transcriptional control of defense genes expression. *Front Plant Sci*, **6**.

Hoagland, D.R. and Arnon, D.I. (1950) The water-culture method for growing plants without soil. *Circular. California agricultural experiment station*, **347**.

Huang, M.K., Zhang, L., Zhou, L.M., Yung, W.S., Li, M.W. and Lam, H.M. (2021) Genomic Features of Open Chromatin Regions (OCRs) in Wild Soybean and Their Effects on Gene Expressions. *Genes-Basel*, **12**.

Ito, Y., Katsura, K., Maruyama, K., Taji, T., Kobayashi, M., Seki, M., Shinozaki, K. and Yamaguchi-Shinozaki, K. (2006) Functional analysis of rice DREB1/CBF-type transcription factors involved in cold-responsive gene expression in transgenic rice. *Plant Cell Physiol*, **47**, 141-153.

Janda, T., Darko, E., Shehata, S., Kovacs, V., Pal, M. and Szalai, G. (2016) Salt acclimation processes in wheat. *Plant Physiol Bioch*, **101**, 68-75.

Jaskiewicz, M., Conrath, U. and Peterhansel, C. (2011) Chromatin modification acts as a memory for systemic acquired resistance in the plant stress response. *Embo Rep*, **12**, 50-55.

Ji, W., Cong, R., Li, S., Li, R., Qin, Z.W., Li, Y.J., Zhou, X.L., Chen, S.X. and Li, J. (2016) Comparative Proteomic Analysis of Soybean Leaves and Roots by iTRAQ Provides Insights into Response Mechanisms to Short-Term Salt Stress. *Front Plant Sci*, **7**.

Jia, Q., Li, M.W., Zheng, C.W., Xu, Y.Y., Sun, S., Li, Z., Wong, F.L., Song, J.L., Lin, W.W., Li, Q.H., Zhu, Y.B., Liang, K.J., Lin, W.X. and Lam, H.M. (2021) The soybean plasma membrane-localized cation/H+ exchanger GmCHX20a plays a negative role under salt stress. *Physiol Plantarum*, **171**, 714-727.

Kim, D., Landmead, B. and Salzberg, S.L. (2015) HISAT: a fast spliced aligner with low memory requirements. *Nat Methods*, **12**, 357-U121.

Lamke, J., Brzezinka, K., Altmann, S. and Baurle, I. (2016) A hit-and-run heat shock factor governs sustained histone methylation and transcriptional stress memory. *Embo J*, **35**, 162-175.

Langfelder, P. and Horvath, S. (2008) WGCNA: an R package for weighted correlation network analysis. *Bmc Bioinformatics*, **9**.

Langmead, B. and Salzberg, S.L. (2012) Fast gapped-read alignment with Bowtie 2. *Nat Methods*, **9**, 357-U354.

Lee, T.A. and Bailey-Serres, J. (2019) Integrative Analysis from the Epigenome to Translatome Uncovers Patterns of Dominant Nuclear Regulation during Transient Stress. *Plant Cell*, **31**, 2573-2595.

Li, H., Handsaker, B., Wysoker, A., Fennell, T., Ruan, J., Homer, N., Marth, G., Abecasis, G., Durbin, R. and Proc, G.P.D. (2009) The Sequence Alignment/Map format and SAMtools. *Bioinformatics*, **25**, 2078-2079.

Liu, A.L., Xiao, Z.X., Li, M.W., Wong, F.L., Yung, W.S., Ku, Y.S., Wang, Q.W., Wang, X., Xie, M., Yim, A.K.Y., Chan, T.F. and Lam, H.M. (2019a) Transcriptomic reprogramming in soybean seedlings under salt stress. *Plant Cell Environ*, **42**, 98-114.

Liu, H.C., Lamke, J., Lin, S.Y., Hung, M.J., Liu, K.M., Charng, Y.Y. and Baurle, I. (2018)

Distinct heat shock factors and chromatin modifications mediate the organ-autonomous transcriptional memory of heat stress. *Plant J*, **95**, 401-413.

Liu, J., Yang, R., Jian, N., Wei, L., Ye, L., Wang, R., Gao, H. and Zheng, Q. (2020) Putrescine metabolism modulates the biphasic effects of brassinosteroids on canola and Arabidopsis salt tolerance. *Plant Cell Environ*, **43**, 1348-1359.

Liu, Y.H., Liu, K.P., Yin, L.F., Yu, Y., Qi, J., Shen, W.H., Zhu, J., Zhang, Y.J. and Dong, A.W. (2019b) H3K4me2 functions as a repressive epigenetic mark in plants. *Epigenet Chromatin*, **12**.

Livak, K.J. and Schmittgen, T.D. (2001) Analysis of relative gene expression data using real-time quantitative PCR and the 2(T)(-Delta Delta C) method. *Methods*, **25**, 402-408.

Love, M.I., Huber, W. and Anders, S. (2014) Moderated estimation of fold change and dispersion for RNA-seq data with DESeq2. *Genome Biol*, **15**.

Lu, P.T., Kang, M., Jiang, X.Q., Dai, F.W., Gao, J.P. and Zhang, C.Q. (2013) RhEXPA4, a rose expansin gene, modulates leaf growth and confers drought and salt tolerance to Arabidopsis. *Planta*, **237**, 1547-1559.

Mauch-Mani, B., Baccelli, I., Luna, E. and Flors, V. (2017) Defense Priming: An Adaptive Part of Induced Resistance. *Annu Rev Plant Biol*, **68**, 485-512.

Mizoi, J., Ohori, T., Moriwaki, T., Kidokoro, S., Todaka, D., Maruyama, K., Kusakabe, K., Osakabe, Y., Shinozaki, K. and Yamaguchi-Shinozaki, K. (2013) GmDREB2A;2, a Canonical DEHYDRATION-RESPONSIVE ELEMENT-BINDING PROTEIN2-Type Transcription Factor in Soybean, Is Posttranslationally Regulated and Mediates Dehydration-Responsive Element-Dependent Gene Expression. *Plant Physiol*, **161**, 346-361.

Moore, J.P., Vicre-Gibouin, M., Farrant, J.M. and Driouich, A. (2008) Adaptations of higher plant cell walls to water loss: drought vs desiccation. *Physiol Plantarum*, **134**, 237-245.

Nguyen, C.T., Agorio, A., Jossier, M., Depre, S., Thomine, S. and Filleur, S. (2016) Characterization of the Chloride Channel-Like, AtCLCg, Involved in Chloride Tolerance in Arabidopsis thaliana. *Plant Cell Physiol*, **57**, 764-775.

Pandolfi, C., Azzarello, E., Mancuso, S. and Shabala, S. (2016) Acclimation improves salt stress tolerance in Zea mays plants. *J Plant Physiol*, **201**, 1-8.

Pandolfi, C., Bazihizina, N., Giordano, C., Mancuso, S. and Azzarello, E. (2017) Salt

acclimation process: a comparison between a sensitive and a tolerant Olea europaea cultivar. *Tree Physiol*, **37**, 380-388.

Pertea, M., Kim, D., Pertea, G.M., Leek, J.T. and Salzberg, S.L. (2016) Transcript-level expression analysis of RNA-seq experiments with HISAT, StringTie and Ballgown. *Nat Protoc*, **11**, 1650-1667.

Phang, T.H., Shao, G.H. and Lam, H.M. (2008) Salt tolerance in soybean. *J Integr Plant Biol*, **50**, 1196-1212.

Qi, X.P., Li, M.W., Xie, M., Liu, X., Ni, M., Shao, G.H., Song, C., Yim, A.K.Y., Tao, Y., Wong, F.L., Isobe, S., Wong, C.F., Wong, K.S., Xu, C.Y., Li, C.Q., Wang, Y., Guan, R., Sun, F.M., Fan, G.Y., Xiao, Z.X., Zhou, F., Phang, T.H., Liu, X., Tong, S.W., Chan, T.F., Yiu, S.M., Tabata, S., Wang, J., Xu, X. and Lam, H.M. (2014) Identification of a novel salt tolerance gene in wild soybean by whole-genome sequencing. *Nat Commun*, **5**.

Quinlan, A.R. and Hall, I.M. (2010) BEDTools: a flexible suite of utilities for comparing genomic features. *Bioinformatics*, **26**, 841-842.

Ramirez, F., Dundar, F., Diehl, S., Gruning, B.A. and Manke, T. (2014) deepTools: a flexible platform for exploring deep-sequencing data. *Nucleic Acids Res*, **42**, W187-W191.

Rosado, A., Schapire, A.L., Bressan, R.A., Harfouche, A.L., Hasegawa, P.M., Valpuesta, V. and Botella, M.A. (2006) The Arabidopsis tetratricopeptide repeat-containing protein TTL1 is required for osmotic stress responses and abscisic acid sensitivity. *Plant Physiol*, **142**, 1113-1126.

Rui, Y. and Dinneny, J.R. (2020) A wall with integrity: surveillance and maintenance of the plant cell wall under stress. *New Phytol*, **225**, 1428-1439.

Russ, J.D., Zaveri, E.D., Damania, R., Desbureaux, S.G., Escurra, J.J. and Rodella, A.S. (2020) *Salt of the earth: quantifying the impact of water salinity on global agricultural productivity* Washington, DC: Word Bank.

Sani, E., Herzyk, P., Perrella, G., Colot, V. and Amtmann, A. (2013) Hyperosmotic priming of Arabidopsis seedlings establishes a long-term somatic memory accompanied by specific changes of the epigenome. *Genome Biol*, **14**.

Schmutz, J., Cannon, S.B., Schlueter, J., Ma, J.X., Mitros, T., Nelson, W., Hyten, D.L., Song, Q.J., Thelen, J.J., Cheng, J.L., Xu, D., Hellsten, U., May, G.D., Yu, Y., Sakurai, T., Umezawa, T., Bhattacharyya, M.K., Sandhu, D., Valliyodan, B., Lindquist, E., Peto,

M., Grant, D., Shu, S.Q., Goodstein, D., Barry, K., Futrell-Griggs, M., Abernathy, B., Du, J.C., Tian, Z.X., Zhu, L.C., Gill, N., Joshi, T., Libault, M., Sethuraman, A., Zhang, X.C., Shinozaki, K., Nguyen, H.T., Wing, R.A., Cregan, P., Specht, J., Grimwood, J., Rokhsar, D., Stacey, G., Shoemaker, R.C. and Jackson, S.A. (2010) Genome sequence of the palaeopolyploid soybean. *Nature*, **463**, 178-183.

Shen, L., Shao, N.Y., Liu, X.C., Maze, I., Feng, J. and Nestler, E.J. (2013) diffReps: Detecting Differential Chromatin Modification Sites from ChIP-seq Data with Biological Replicates. *Plos One*, **8**.

Shen, X.Y., Wang, Z.L., Song, X.F., Xu, J.J., Jiang, C.Y., Zhao, Y.X., Ma, C.L. and Zhang, H. (2014) Transcriptomic profiling revealed an important role of cell wall remodeling and ethylene signaling pathway during salt acclimation in Arabidopsis. *Plant Mol Biol*, **86**, 303-317.

Song, Y.G., Ji, D.D., Li, S., Wang, P., Li, Q. and Xiang, F.N. (2012) The Dynamic Changes of DNA Methylation and Histone Modifications of Salt Responsive Transcription Factor Genes in Soybean. *Plos One*, **7**.

Sun, L., Song, G.S., Guo, W.J., Wang, W.X., Zhao, H.K., Gao, T.T., Lv, Q.X., Yang, X., Xu, F., Dong, Y.S. and Pu, L. (2019) Dynamic Changes in Genome-Wide Histone3 Lysine27 Trimethylation and Gene Expression of Soybean Roots in Response to Salt Stress. *Front Plant Sci*, **10**.

Sun, Y.H., Zhao, J., Li, X.Y. and Li, Y.Z. (2020) E2 conjugases UBC1 and UBC2 regulate MYB42-mediated SOS pathway in response to salt stress in Arabidopsis. *New Phytol*, **227**, 455-472.

Teakle, N.L. and Tyerman, S.D. (2010) Mechanisms of Cl- transport contributing to salt tolerance. *Plant Cell Environ*, **33**, 566-589.

Tenhaken, R. (2015) Cell wall remodeling under abiotic stress. *Front Plant Sci*, **5**.

Tian, T., Liu, Y., Yan, H.Y., You, Q., Yi, X., Du, Z., Xu, W.Y. and Su, Z. (2017) agriGO v2.0: a GO analysis toolkit for the agricultural community, 2017 update. *Nucleic Acids Res*, **45**, W122-W129.

Ueda, M., Matsui, A., Tanaka, M., Nakamura, T., Abe, T., Sako, K., Sasaki, T., Kim, J.M., Ito, A., Nishino, N., Shimada, H., Yoshida, M. and Seki, M. (2017) The Distinct Roles of Class I and II RPD3-Like Histone Deacetylases in Salinity Stress Response. *Plant*

Physiol, **175**, 1760-1773.

Umezawa, T., Nakashima, K., Miyakawa, T., Kuromori, T., Tanokura, M., Shinozaki, K. and Yamaguchi-Shinozaki, K. (2010) Molecular Basis of the Core Regulatory Network in ABA Responses: Sensing, Signaling and Transport. *Plant Cell Physiol*, **51**, 1821-1839.

Umezawa, T., Shimizu, K., Kato, M. and Ueda, T. (2000) Enhancement of salt tolerance in soybean with NaCl pretreatment. *Physiol Plantarum*, **110**, 59-63.

van Zelm, E., Zhang, Y.X. and Testerink, C. (2020) Salt Tolerance Mechanisms of Plants. *Annual Review of Plant Biology, Vol 71, 2020*, **71**, 403-433.

Wang, H.M., Zhou, L., Fu, Y.P., Cheung, M.Y., Wong, F.L., Phang, T.H., Sun, Z.X. and Lam, H.M. (2012) Expression of an apoplast-localized BURP-domain protein from soybean (GmRD22) enhances tolerance towards abiotic stress. *Plant Cell Environ*, **35**, 1932-1947.

Wang, Q.W., Yung, W.S., Wang, Z.L. and Lam, H.M. (2020) The histone modification H3K4me3 marks functional genes in soybean nodules. *Genomics*, **112**, 5282-5294.

Wang, X.F., Elling, A.A., Li, X.Y., Li, N., Peng, Z.Y., He, G.M., Sun, H., Qi, Y.J., Liu, X.S. and Deng, X.W. (2009) Genome-Wide and Organ-Specific Landscapes of Epigenetic Modifications and Their Relationships to mRNA and Small RNA Transcriptomes in Maize. *Plant Cell*, **21**, 1053-1069.

Wang, X.J., Guo, C., Peng, J., Li, C., Wan, F.F., Zhang, S.M., Zhou, Y.Y., Yan, Y., Qi, L.J., Sun, K.W., Yang, S.H., Gong, Z.Z. and Li, J.G. (2019) ABRE-BINDING FACTORS play a role in the feedback regulation of ABA signaling by mediating rapid ABA induction of ABA co-receptor genes. *New Phytol*, **221**, 341-355.

Wei, P.P., Wang, L.C., Liu, A.L., Yu, B.J. and Lam, H.M. (2016) GmCLC1 Confers Enhanced Salt Tolerance through Regulating Chloride Accumulation in Soybean. *Front Plant Sci*, **7**.

Wickham, H. (2009) ggplot2: Elegant Graphics for Data Analysis. *Use R*, 1-212.

Wojtaszek, P. (1997) Oxidative burst: An early plant response to pathogen infection. *Biochem J*, **322**, 681-692.

Xie, C., Mao, X.Z., Huang, J.J., Ding, Y., Wu, J.M., Dong, S., Kong, L., Gao, G., Li, C.Y. and Wei, L.P. (2011) KOBAS 2.0: a web server for annotation and identification of enriched pathways and diseases. *Nucleic Acids Res*, **39**, W316-W322.

Xie, Z.L., Nolan, R.O.R., Jiang, H., Tang, B.Y., Zhang, M.C., Li, Z.H. and Yin, Y.H. (2019) The AP2/ERF Transcription Factor TINY Modulates Brassinosteroid-Regulated Plant

Growth and Drought Responses in Arabidopsis. *Plant Cell*, **31**, 1788-1806.

Xu, X.P., Chen, C.H., Fan, B.F. and Chen, Z.X. (2006) Physical and functional interactions between pathogen-induced Arabidopsis WRKY18, WRKY40, and WRKY60 transcription factors. *Plant Cell*, **18**, 1310-1326.

Yamaguchi, N., Matsubara, S., Yoshimizu, K., Seki, M., Hamada, K., Kamitani, M., Kurita, Y., Nomura, Y., Nagashima, K., Inagaki, S., Suzuki, T., Gan, E.S., To, T., Kakutani, T., Nagano, A.J., Satake, A. and Ito, T. (2021) H3K27me3 demethylases alter HSP22 and HSP17.6C expression in response to recurring heat in Arabidopsis. *Nat Commun*, **12**.

Yoshida, T., Mogami, J. and Yamaguchi-Shinozaki, K. (2014) ABA-dependent and ABA-independent signaling in response to osmotic stress in plants. *Curr Opin Plant Biol*, **21**, 133-139.

Yu, Y.C., Wang, N., Hu, R.B. and Xiang, F.N. (2016) Genome-wide identification of soybean WRKY transcription factors in response to salt stress. *Springerplus*, **5**.

Yung, W.S., Li, M.W., Sze, C.C., Wang, Q.N. and Lam, H.M. (2021) Histone modifications and chromatin remodelling in plants in response to salt stress. *Physiol Plantarum*.

Zheng, M., Liu, X.B., Lin, J.C., Liu, X.Y., Wang, Z.Y., Xin, M.M., Yao, Y.Y., Peng, H.R., Zhou, D.X., Ni, Z.F., Sun, Q.X. and Hu, Z.R. (2019) Histone acetyltransferase GCN5 contributes to cell wall integrity and salt stress tolerance by altering the expression of cellulose synthesis genes. *Plant J*, **97**, 587-602.

Zorb, C., Geilfus, C.M. and Dietz, K.J. (2019) Salinity and crop yield. *Plant Biol (Stuttg)*, **21 Suppl 1**, 31-38.

Figure Legends

Figure 1. Effects of high salinity stress on primed and non-primed seedlings.

(A) Phenotypes of soybean seedlings at 1 h with or without high salt (0.9% NaCl) treatment. The primed seedlings were pretreated with mild salt stress (0.3% NaCl) for 6 days, whereas the non-primed seedlings were grown under normal condition for the same period.

(B) and (C) Photosynthetic performance of non-primed and primed seedlings as represented by photosynthetic assimilation rate (B) and stomatal conductance (C) at 0 d and 2 d after high salinity treatment. The data are presented as mean ± SE ($n \geq 4$). Similar trends were observed in two other independent experiments.

(D) Na^+/K^+ ratio in leaves of non-primed and primed seedlings at 0 d and 3 d after high salinity treatment. The data are presented as mean ± SE ($n = 8$). A similar trend was observed in an independent experiment.

(E) Proline content in leaves and roots of non-primed and primed seedlings at 0 d and 3 d after high salinity treatment. The data are presented as mean ± SE ($n = 4$). Similar trends were observed in two other independent experiments.

Statistical analyses in (B) to (E) were performed using one-way analysis of variance (ANOVA) followed by Tukey's post-hoc test at $p < 0.05$. The groups with significant differences are labeled with different letters.

Figure 2. The relationship between histone modifications and gene expressions.

(A) and (B) Metaplots showing the distributions of the ChIP-seq signals of three histone marks (H3K4me2, H3K4me3 and H3K9ac) along the genes in leaves (A) and roots (B) of primed seedlings. Genes were ranked according to the FPKM (fragments per kilobase of transcripts per million mapped reads) values in the RNA-seq data and split into ten groups. TSS, transcription start site; TES, transcription end site.

(C) Numbers of DRG-DEGs that were either up- or down-regulated in leaves and roots between primed and non-primed seedlings. Genes with differential levels of histone marks (H3K4me2, H3K4me3 and H3K9ac) after pretreatment (DRGs) and differential expressions (DEGs) in the predicted directions matching the histone marks in the subsequent salt stress (DRG-DEGs) were identified. Up, genes with lower H3K4me2/higher H3K4me3/higher H3K9ac levels and upregulated transcription. Down, genes with higher H3K4me2/lower H3K4me3/lower H3K9ac levels and downregulated transcription. * Indicates $p < 0.001$ (Hypergeometric test).

(D) Representative snapshots of two selected genes and their histone modification (H3K4me2, H3K4me3 and H3K9ac) statuses and expression in the leaves and roots of non-primed (N) and primed seedlings (P).

Similar trends were observed in other replicates.

(E) Gene ontology (GO) enrichment analysis of DRG-DEGs modified by different histone marks (H3K4me2, H3K4me3 and H3K9ac). For simplicity, only several important GO terms related to stress responses are displayed. The full list of enriched GO terms can be found in Data Set S6. Up, enrichment in genes with lower H3K4me2/higher H3K4me3/higher H3K9ac levels and upregulated transcription. Down, enrichment in genes with higher H3K4me2/lower H3K4me3/lower H3K9ac levels and downregulated transcription. Up and down, enrichment in both up- and downregulated DRG-DEGs.

Figure 3. Heatmaps showing the differentially expressed genes (DEGs) related to the drought-responsive pathway and ion homeostasis in leaves.

The $\log_2$ fold-change in FPKM (fragments per kilobase of transcripts per million mapped reads) values between primed and non-primed seedlings at 0 h, 0.5 h, 1 h, 2 h, 8 h and 24 h after high salinity stress were used to generate the heatmaps. The DEGs in leaves related to the ABA-dependent, ABA-independent pathways and ion homeostasis are shown in (A), (B) and (C), respectively. The DEGs are clustered into sub-families according to their homologs in *Arabidopsis*. Alterations in histone marks (H3K4me2, H3K4me3 or H3K9ac) matching their predicted roles in transcriptional regulation are also displayed. The color scale applies to the heatmaps in all panels.

Figure 4. Heatmaps showing the differentially expressed genes (DEGs) related to the drought-responsive pathway and ion homeostasis in roots.

The $\log_2$ fold-change in FPKM (fragments per kilobase of transcripts per million mapped reads) values between primed and non-primed seedlings at 0 h, 0.5 h, 1 h, 2 h, 8 h and 24 h after high salinity stress were used to generate the heatmaps. The DEGs in roots related to the ABA-dependent, ABA-independent pathways and ion homeostasis are shown in (A), (B) and (C), respectively. The DEGs are clustered into sub-families according to their homologs in *Arabidopsis*. Alterations in histone marks (H3K4me2, H3K4me3 or H3K9ac) matching their predicted roles in transcriptional regulation are also displayed. The color scale applies to the heatmaps in all panels.

Figure 5. Transcriptional modulation of differentially expressed genes (DEGs) in leaves by different transcription factor (TF) families.

(A) Enrichment analysis of the *cis*-elements (ABRE, DRE, GCC-box, and W-box) in the 2,000-bp upstream regions of the upregulated (Up) or downregulated (Down) genes between primed and non-primed seedlings in leaves at 0 h, 0.5 h, 1 h, 2 h, 8 h and 24 h after high salinity stress. Hypergeometric tests were conducted

and the -$\log_{10}$(p-value) of the significantly enriched motifs are shown at each time point. ns, not significant at $p < 0.05$.

(B) Examples of transcriptional networks enriched with downregulated genes between primed and non-primed seedlings in leaves at 0.5 h or 1 h after high salinity stress. The genes encoding WRKY transcription factors are highlighted. The triangles indicate downregulated genes and the squares indicate downregulated genes marked by differential histone modifications (DRG-DEGs) that potentially inhibit transcription. The three *WRKY*s are *GmWRKY29* (*Glyma.04G054200*), *GmWRKY57* (*Glyma.06G142000*) and *GmWRKY85* (*Glyma.08G218600*). The gene names were assigned according to a previous publication (Yu *et al.*, 2016).

Figure 6. Effects of Trichostatin A (TSA) pretreatment on the transcriptional responses of soybean seedlings under high salinity stress.

(A) TSA was used for the 6-day pretreatment of non-primed seedlings. The photosynthetic rates of TSA-treated seedlings at 2 h after high salinity stress was compared to those of non-primed, unpretreated seedlings and primed seedlings. The data were analyzed for statistical significance by one-way ANOVA followed by Tukey's post-hoc test, and are presented as mean ± SE (n = 3). The groups with significant differences ($p < 0.05$) are labeled with different letters. A similar trend was observed in another independent experiment.

(B) The enrichment levels of H3K9ac at *GmCLC1*, *ARF16-* (*Glyma.20G180000*), *PP2C68-* (*Glyma.19G147800*) and *SCR-related* (*Glyma.18G220100*) in roots of non-primed, unpretreated (white), non-primed, TSA-treated (grey) and primed (black) seedlings after the 6-day pretreatment were analyzed by ChIP-qPCR. The H3K9ac level in non-primed, unpretreated seedlings was set to 1. The data are presented as mean ± SD (n ≥ 3). Statistical differences between non-primed seedlings with or without TSA pretreatment were determined using Student's t test (*$p < 0.05$ ***$p < 0.001$).

(C) The relative expression levels of the selected genes in non-primed, unpretreated (white), non-primed, TSA-treated (grey) and primed (black) seedlings at 0 h and 0.5 h after high salinity stress were analyzed by RT-qPCR. The data are presented as mean ± SD (n ≥ 3). Statistical differences between non-primed seedlings with or without TSA pretreatment were determined using Student's t test (*$p < 0.05$, **$p < 0.01$, ***$p < 0.001$). A similar trend was observed in another independent experiment. *Bic-C2* and *F-box protein2* were used as the reference genes.

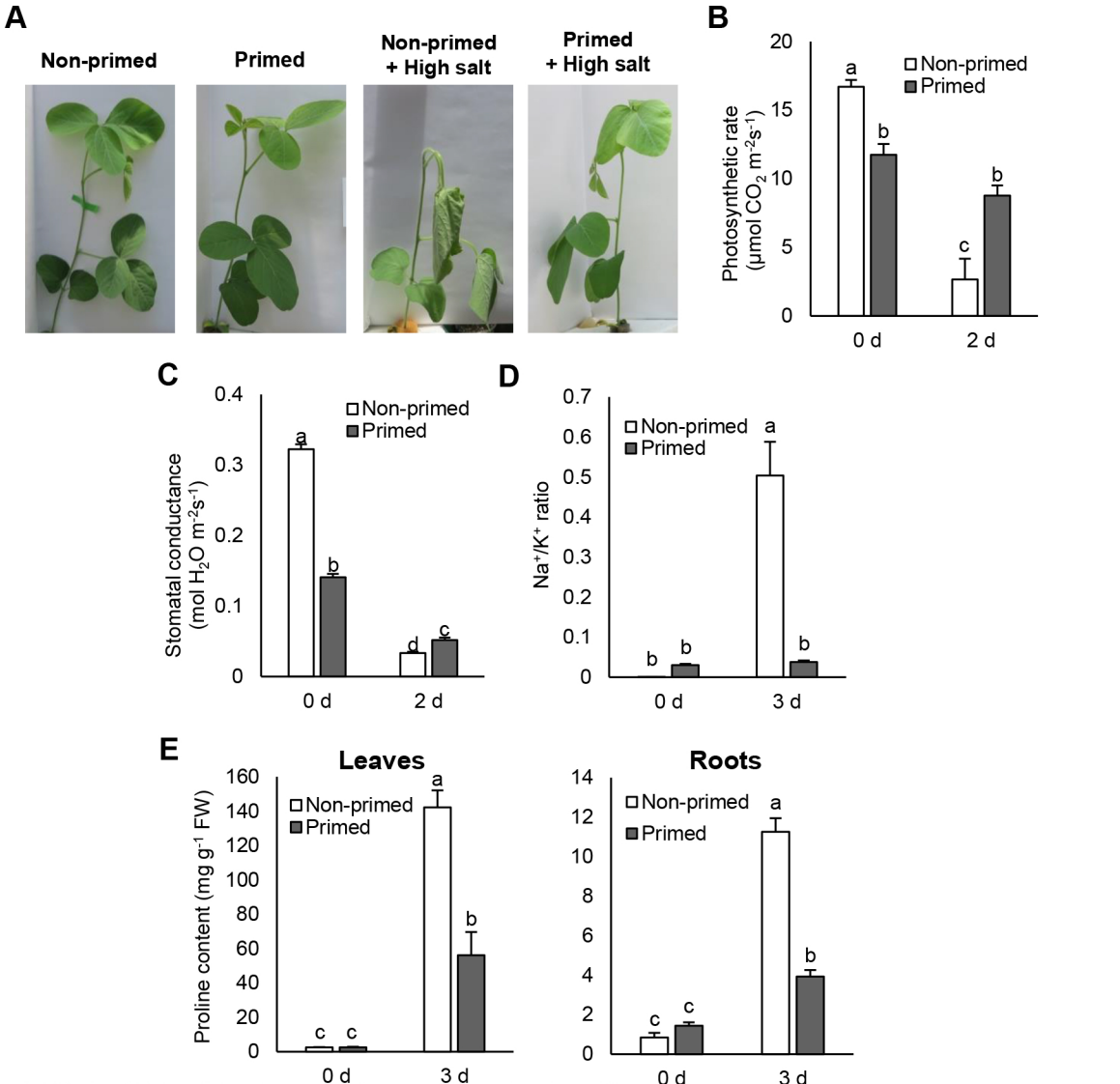

Figure 1. Effects of high salinity stress on primed and non-primed seedling.
(A) Phenotypes of soybean seedlings at 1 h with or without high salt (0.9% NaCl) treatment. The primed seedlings were pretreated with mild stress (0.3% NaCl) for 6 days, whereas the non-primed seedlings were grown under normal condition for the same period.
(B) and (C) Photosynthetic performance of non-primed and primed seedlings was measured as the photosynthetic assimilation rate (B) and stomatal conductance (C) at 0 d and 2 d after high salinity treatment. The data are presented as mean ± SE (n ≥ 4). Similar trends were observed in two other independent experiments.
(D) Na^+/K^+ ratio in leaves of non-primed and primed seedlings at 0 d and 3 d after high salinity treatment. The data are presented as mean ± SE (n = 8). A similar trend was observed in an independent experiment.
(E) Proline content in leaves and roots of non-primed seedlings and primed seedlings at 0 d and 3 d after high salinity treatment. The data are presented as mean ± SE (n = 4). Similar trends were observed in two other independent experiments.
Statistical analyses in (B) to (F) were performed using one-way analysis of variance followed by Tukey's post-hoc test at $p < 0.05$. The groups with significant differences are labeled with different letters.

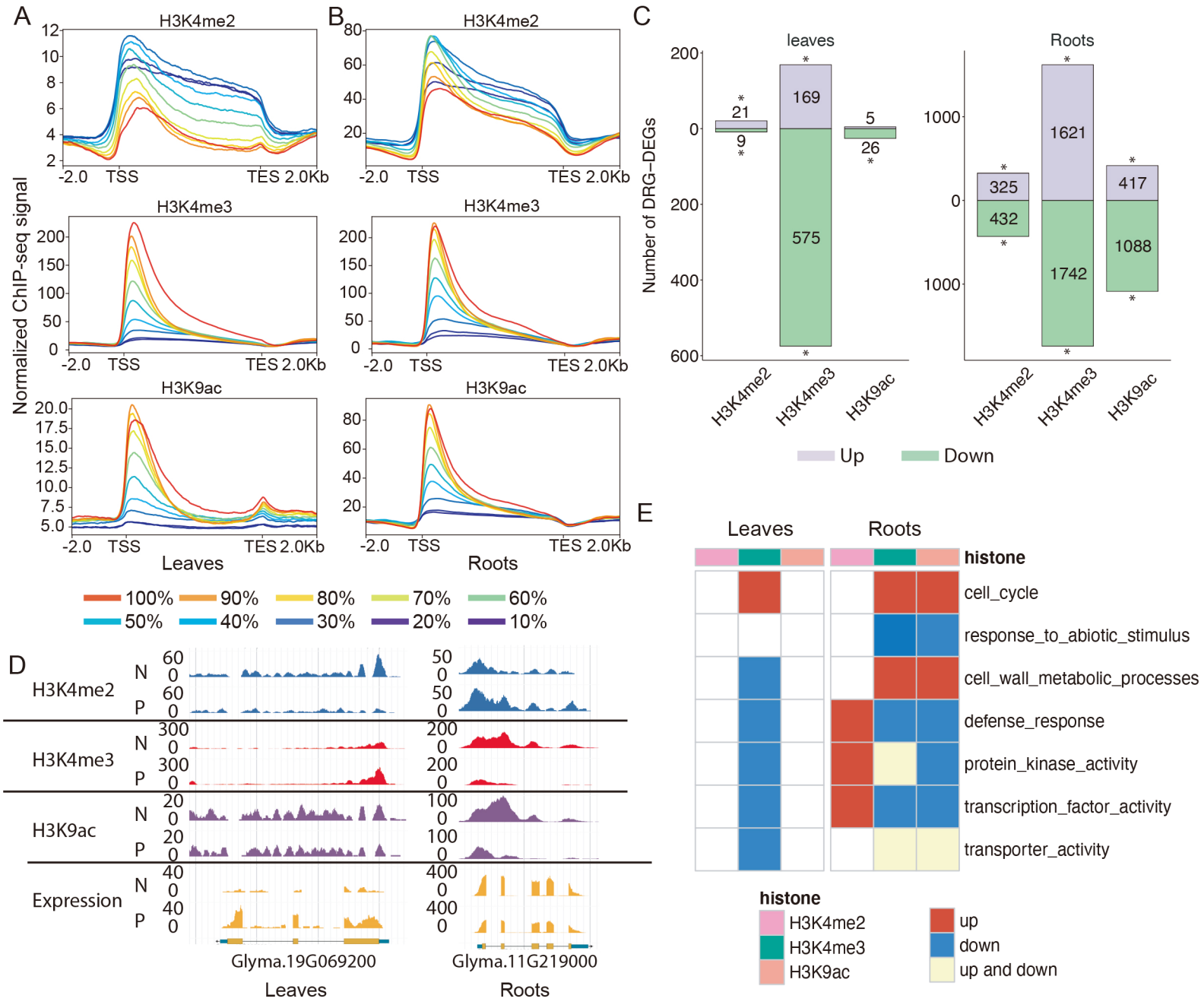

Figure 2. The relationship between histone modifications and gene expressions.
(A) and (B) Metaplots showing the distributions of the ChIP-seq signals of three histone marks (H3K4me2, H3K4me3 and H3K9ac) along the genes in leaves (A) and roots (B) of primed seedlings. Genes were ranked according to the FPKM (fragments per kilobase of transcripts per million mapped reads) values in the RNA-seq data and split into ten groups. TSS, transcription start site; TES, transcription end site.
(C) Numbers of DRG-DEGs that were either up- or down-regulated in leaves and roots between primed and non-primed seedlings. Genes with differential levels of histone marks (H3K4me2, H3K4me3 and H3K9ac) after pretreatment (DRGs) and differential expressions (DEGs) in the predicted directions matching the histone marks in the subsequent salt stress (DRG-DEGs) were identified. Up, genes with lower H3K4me2/higher H3K4me3/higher H3K9ac levels and upregulated transcription. Down, genes with higher H3K4me2/lower H3K4me3/lower H3K9ac levels and downregulated transcription. *Indicates $p < 0.001$ (Hypergeometric test).
(D) Representative snapshots of two selected genes and their histone modification (H3K4me2, H3K4me3 and H3K9ac) statuses and expression in the leaves and roots of non-primed (N) and primed seedlings (P). Similar trends were observed in other replicates.
(E) Gene ontology (GO) enrichment analysis of DRG-DEGs modified by different histone marks (H3K4me2, H3K4me3 and H3K9ac). For simplicity, only several important GO terms related to stress responses are displayed. The full list of enriched GO terms can be found in Data Set S6. Up, enrichment in genes with lower H3K4me2/higher H3K4me3/higher H3K9ac levels and upregulated transcription. Down, enrichment in genes with higher H3K4me2/lower H3K4me3/lower H3K9ac levels and downregulated transcription. Up and down, enrichment in both up- and downregulated DRG-DEGs.

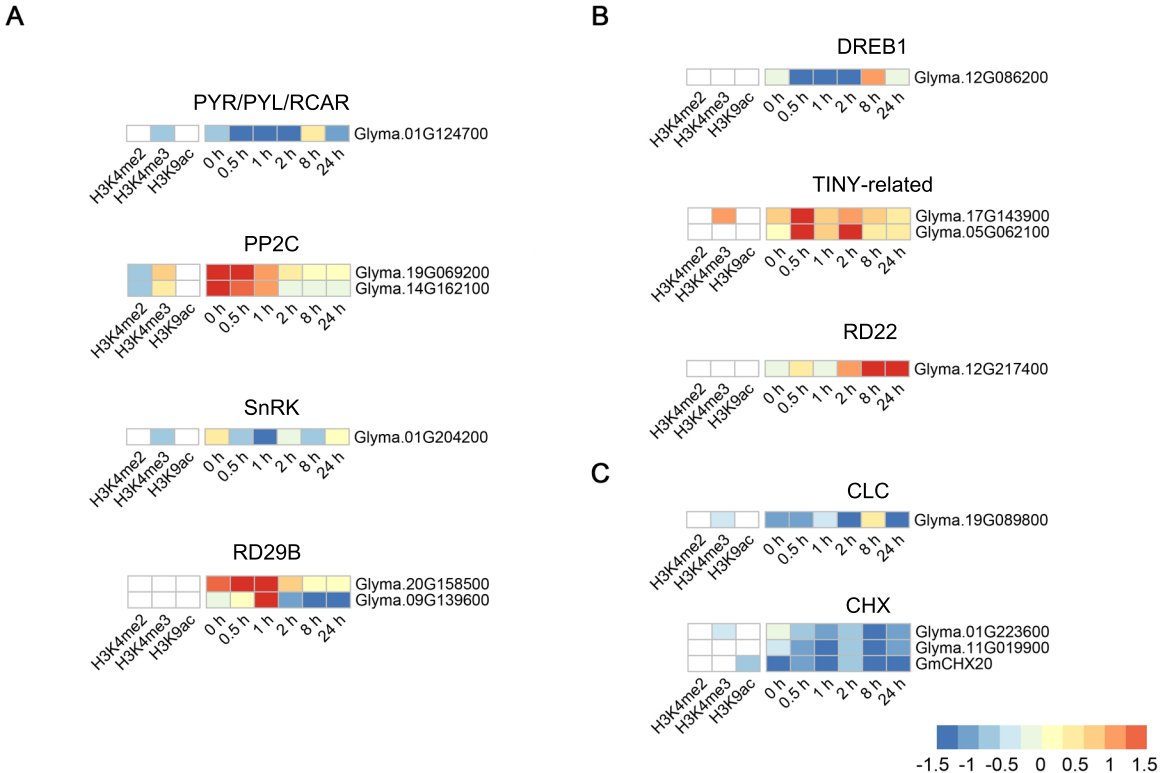

Figure 3. Heatmaps showing the differentially expressed genes (DEGs) related to the drought-responsive pathway and ion homeostasis in leaves. The $\log_2$ fold-change in FPKM (fragments per kilobase of transcripts per million mapped reads) values between primed and non-primed seedlings at 0 h, 0.5 h, 1 h, 2 h, 8 h and 24 h after high salinity stress were used to generate the heatmaps. The DEGs in leaves related to the ABA-dependent , ABA-independent pathways and ion homeostasisare shown in (A), (B) and (C), respectively. The DEGs are clustered into sub-families according to their homologs in *Arabidopsis*. Alterations in histone marks (H3K4me2, H3K4me3 or H3K9ac) matching their predicted roles in transcriptional regulation are also displayed. The color scale applies to the heatmaps in all panels.

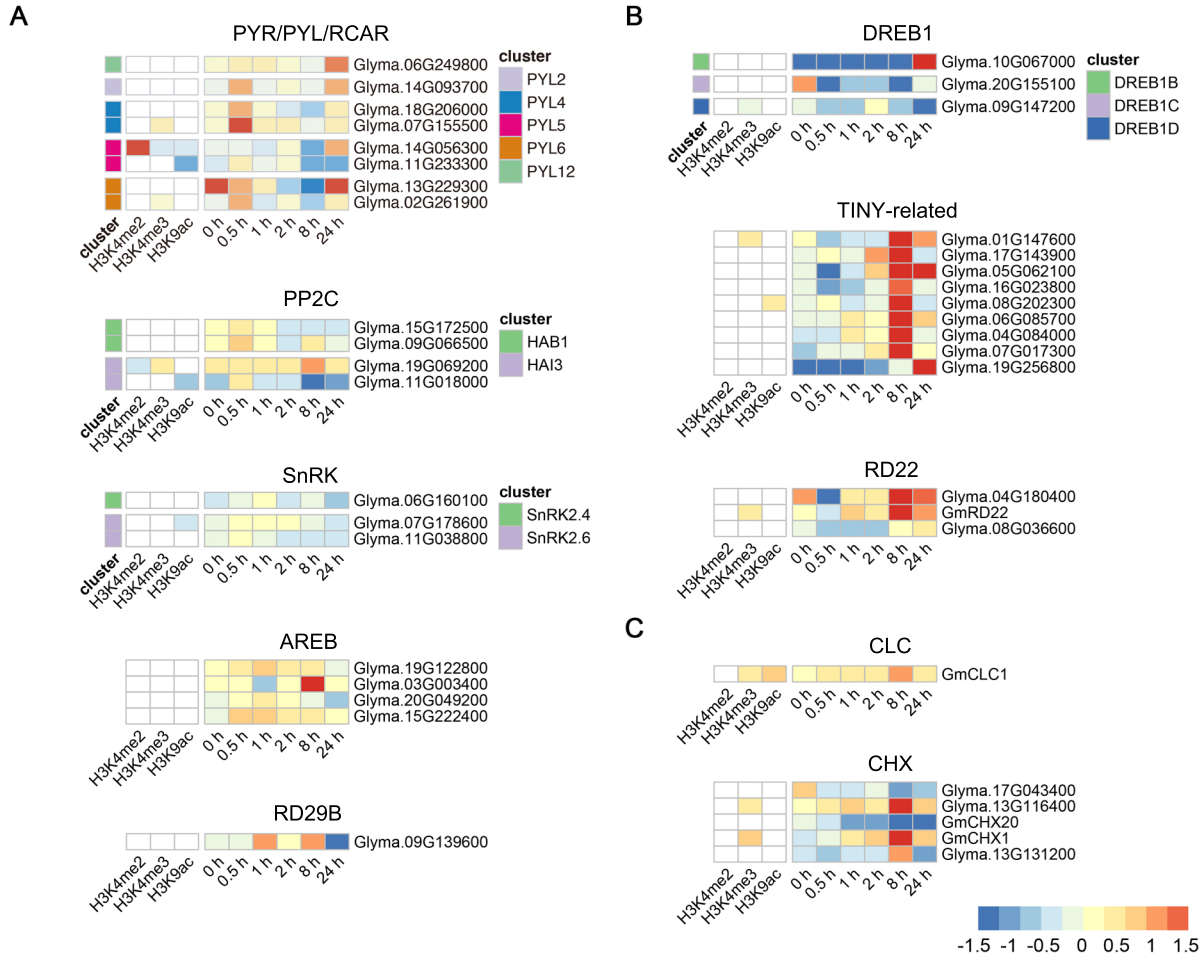

Figure 4. Heatmaps showing the differentially expressed genes (DEGs) related to the drought-responsive pathway and ion homeostasis in roots. The $\log_2$ fold-change in FPKM (fragments per kilobase of transcripts per million mapped reads) values between primed and non-primed seedlings at 0 h, 0.5 h, 1 h, 2 h, 8 h and 24 h after high salinity stress were used to generate the heatmaps. The DEGs related to the ABA-dependent, ABA-independent pathways and ion homeostasis are shown in (A), (B) and (C), respectively. The DEGs are clustered into sub-families according to their homologs in *Arabidopsis*. Alterations in histone marks (H3K4me2, H3K4me3 or H3K9ac) matching their predicted roles in transcriptional regulation are also displayed. The color scale applies to the heatmaps in all panels.

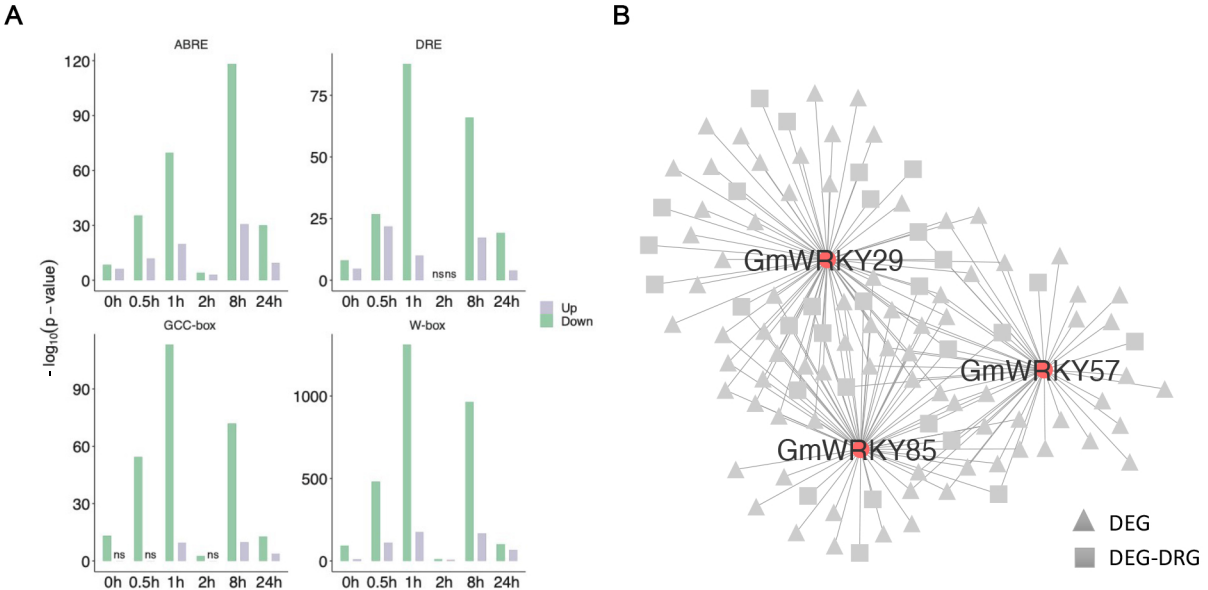

Figure 5. Transcriptional modulation of the differentially expressed genes (DEGs) in leaves by different transcription factor (TF) families.

(A) Enrichment analysis of the *cis*-elements (ABRE, DRE, GCC-box,and W-box) in the 2,000 bp upstream regions of the upregulated (Up) or downregulated (Down) genes between primed and non-primed seedlings in leaves at 0 h, 0.5 h, 1 h, 2 h, 8 h and 24 h after high salinity stress. Hypergeometric tests were conducted and the $-\log_{10}$(p-value) of the significantly enriched motifs are shown at each time point. ns, not significant at $p < 0.05$.

(B) Examples of transcriptional networks enriched with downregulated genes between primed and non-primed seedlings in leaves at 0.5 h or 1 h after high salinity stress.The genes encoding WRKY transcription factors are highlighted. The triangles indicate downregulated genes and the squares indicate downregulated genes marked by differential histone modifications (DRG-DEGs) that potentially inhibit transcription. The three *WRKYs* are *GmWRKY29* (*Glyma.04G054200*), *GmWRKY57* (*Glyma.06G142000*) and *GmWRKY85* (*Glyma.08G218600*). The gene names were assigned according to a previous publication (Yu et al., 2016).

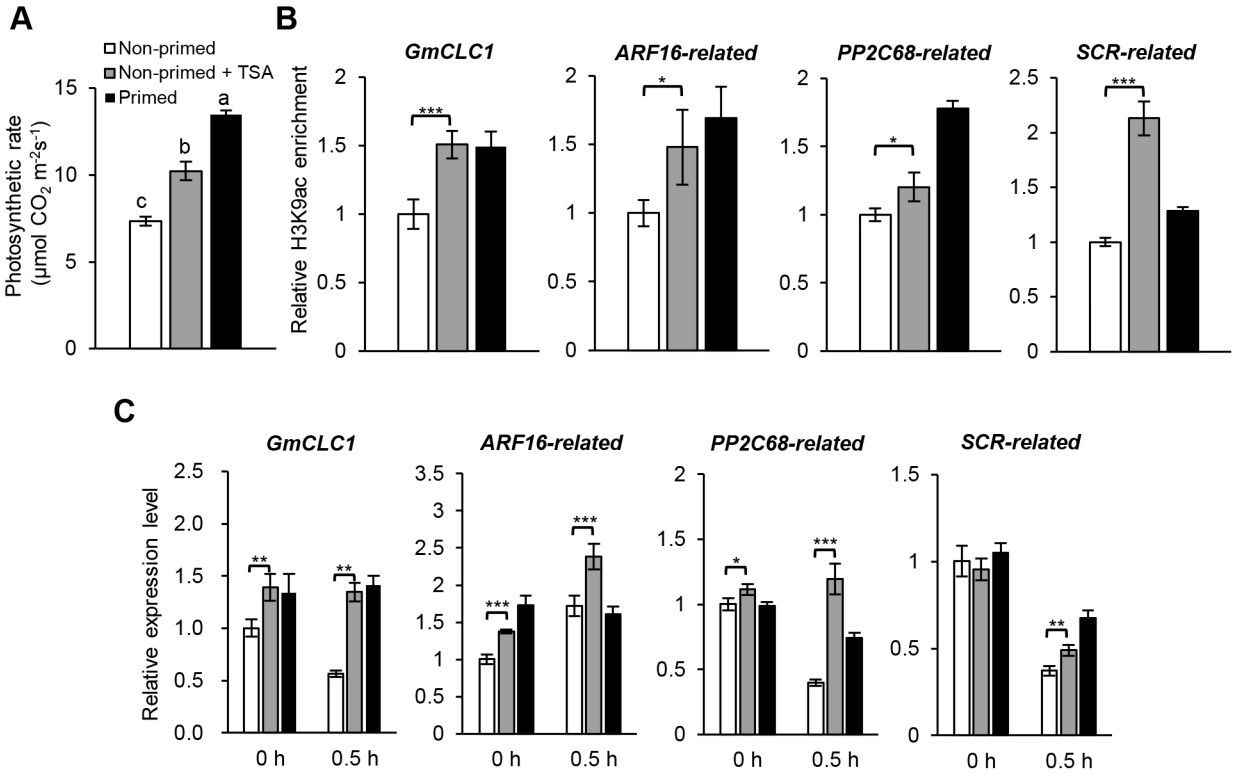

Figure 6. Effects of Trichostatin A (TSA) pretreatment on the transcriptional responses of soybean seedlings under high salinity stress.

(A) TSA was used for the 6-day pretreatment of non-primed seedlings. The photosynthetic rates of TSA-treated seedlings at 2 h after high salinity stress was compared to those of non-primed, unpretreated seedlings and primed seedlings. The data were analyzed for statistical significance by one-way ANOVA followed by Tukey's post-hoc test, and are presented as mean ± SE ($n = 3$). The groups with significant differences ($p < 0.05$) are labeled with different letters. A similar trend was observed in another independent experiment.

(B) The enrichment levels of H3K9ac at *GmCLC1*, *ARF16-* (*Glyma.20G180000*), *PP2C68-* (*Glyma.19G147800*) and *SCR-related* (*Glyma.18G220100*) in roots of non-primed, unpretreated (white), non-primed, TSA-treated (grey) and primed (black) seedlings after the 6-day pretreatment were analyzed by ChIP-qPCR. The H3K9ac level in non-primed, unpretreated seedlings was set to 1. The data are presented as mean ± SD ($n \geq 3$). Statistical differences between non-primed seedlings with or without TSA pretreatment were determined using Student's t test (*$p < 0.05$ ***$p < 0.001$).

(C) The relative expression levels of the selected genes in non-primed, unpretreated (white), non-primed, TSA-treated (grey) and primed (black) seedlings at 0 h and 0.5 h after high salinity stress were analyzed by RT-qPCR. The data are presented as mean ± SD ($n \geq 3$). Statistical differences between non-primed seedlings with or without TSA pretreatment were determined using Student's t test (*$p < 0.05$, **$p < 0.01$, ***$p < 0.001$). A similar trend was observed in another independent experiment. *Bic-C2* and *F-box protein2* were used as the reference genes.